Cementless Acetabular Revision with Rim Acetabular Defects: Experimental and FEA Investigation

By

MARK H. GONZALEZ

MD: University of Chicago

BS Biochemistry: University of Illinois Champaign Urbana

MEng: University of Illinois Chicago

THESIS

Submitted as a partial fulfillment of the requirements

for the degree of Doctor of Philosophy in Mechanical Engineering

in the Graduate College of the

University of Illinois at Chicago, 2014

Chicago, Illinois

Defense Committee:

Farid Amirouche, PhD (Advisor)

Thomas Royston, PhD

Sabri Cetinkunt, PhD

Michael Scott, PhD

Alfonso Mejia, MD, MPH

Acknowledgements

Frank Gonzalez; My dad: A real engineer who could design, fix or build anything. He taught me to think like an engineer.

Dawn My wife: Your positive attitude and spirit continue to be an inspiration.

Elena Isabel and Marko: My children who have missed their dad while I studied and who make it all worthwhile.

Farid Amirouche: Farid is a close friend and a great adviser. He convinced me that I could be an engineer. He pushed me to complete this thesis and without him I could never have done it.

Ivan Zivkovich: We worked together on the early testing of the cadaver bone interface. Ivan was a gentleman, a great engineer and a fine friend.

Gianfranco Solitro: Gianfranco is a great friend and a great engineer who helped me learn how to mesh.

Members of the committee; Thank you for your time and your kindness

Al Mejia:
Sabri Cetinkunt
Michael Scott
Thomas Royston

MHG

Table of Contents

List of Tables

List of Figures

Summary

Total Hip Arthroplasty (THA) has become a very popular procedure in the world today. As people are living longer and requiring improved function, the indications and frequency of performing total hip arthroplasty have expanded. As a result there are an increasing number of patients who have failed total hip arthroplasties that need revision. Failure generally occurs as a result of the biological response to wear particles. Polyethylene particles are generates by frictional wear both at the articulation between the femoral head and the polyethylene liner and between the liner and the metal cup. The particles are opsonized by macrophages initiating a cascade that causes acetabular bone loss as a result the acetabular implant loosens and has to be revised.

The challenge to the surgeon is to place a new acetabular implant in the bone deficient acetabulum. Other causes of bone loss about the acetabulum include congenitally or developmentally dislocated hips and trauma about the hip.

Our purpose is to better understand acetabular wall (rim) defects, and the acetabular bone cup interface stability and fixation. To this end several FEA models will be developed to investigate the different scenarios involved in THA in the presence of rim defects.

The first step is to create and validate a FEA Model. A cadaver pelvis is implanted with acetabular cups bilaterally. On one side a defect is created in the pelvis. Each construct is loaded with a physiologic load followed by a supraphysiologic load and the micromotion of the cups noted. Based on Ct scans a model is created of both hemipelvis acetabular cups are implanted virtually. Boundary conditions are generated based on the previous literature and each pelvis is loaded with a profile identical to the experimental profile.

Once the model is validated the model is used to examine three scenarios that will provide information to the hip surgeon contemplating hip revision in the case of bone deficiency.

The scenarios are 1: The effect of the varying degrees of cup fixation on cup stability. 2: The effect of defect position on cup stability, 3: The effect of defect size and cup stability.

The results show that the cup stability is sensitive to the degree of equatorial fixation. Decreasing the fixation especially on the rim side can greatly increase the micromotion of a cup under physiologic stress. The position of a defect is critical. Defects that are superior or inferior and are outside the anterior and posterior columns have a minimal effect on cup stability. Defects of the anterior or posterior columns create instability and are sensitive to size of defect.

CHAPTER 1 - Introduction

The cementless total hip arthroplasty has revolutionized total hip arthroplasty around the world [1]. As the number of patients with total hip arthroplasty increases the number of patient with a failed total hip arthroplasty will increase [2] [3].

The cementless total hip creates fixation by bone ingrowth into a porous metal surface. It has been demonstrated that bone will grow into a porous surface with pore size of 50 to 400 microns [4]. For ingrowth to occur less than 50 microns of micromotion is necessary between the bone and the porous metal surface.

To create rigid fixation between the acetabular cup and the acetabulum the acetabulum is reamed with hemispherical reamers and a cup is implanted which is 1-2 mm larger in diameter than the reamed acetabulum. The acetabular cup is then hammered in an anatomic position. This is termed underreaming.

In general in an acetabulum with moderate to severe arthritis the press fit fixation of the acetabular cup is adequate and bone ingrowth occurs creating a durable long lasting acetabular implant. In certain situations initial fixation can be less than ideal because of a bone deficiency. Common causes of bone deficiency are previous failure of a total hip arthroplasty, developmental dysplasia of the hip and trauma.

In the situation where there are bone deficiencies of the acetabulum, underreaming and placement of a cup may not be a rigid construct. There are two physical factors that determine this. The underreamed cup creates a hoop stress in the rim of the acetabulum creating a compressive force on the rim of the cup. This compressive force creates a friction force

between the cup and bone. The degree of friction is determined by the friction coefficient of the cup bone interface and normal compressive force between the two surfaces. When the bone rim is deficient the rim can expand with less force diminishing the compressive force. The second factor is physical contact between the cup and bone. Bone deficiencies can lead to decreased contact, which also diminishes the frictional force.

If the interface between the cup and the bone is not rigid, when the cup is loaded micromotion can occur. When this micromotion exceeds 50 to 100 microns, this can preclude bony ingrowth at the interface. In this scenario fibrous ingrowth occurs which can cause pain and eventually lead to cup failure.

In the situation where there is bone deficiency of an acetabulum, the surgeon must place an acetabular cup with adjunctive fixation to stabilize the cup. Options include the use of screws, bone augments, bi-lobed cups, flanged cups with screws and completely custom made cups.

An understanding of the mechanics of cup stability can help the surgeon in planning a revision construct.

To further investigate cup stability in the face of a bone defect a mathematical model of the pelvis and specifically the cup bone interface was created. A model will be created based on a patient specific CT scan with MIMICS. The model will then be imported into a CAD program to create the bone defects. The model will then be imported into ANSYS for FEA. The Acetabular cup will be loaded with a combined profile of torque and compression to mimic the gait cycle. The same cadaver will be operated on and an acetabular cup placed surgically. The cup will be loaded with the same loading profile. The model will be validated comparing the two micromotion profiles of the real and the virtual experiment.

The purpose of creating the validated model is to measure micromotion of a cup bone construct and the stresses involved. Three specific questions will be posed. 1. How does the size of a bone defect influence cup stability. 2: How does position of a bone defect influence cup stability. 3: How does the degree of cup fixation influence the cup stability.

The current research is unique as it is the one of the first attempts to understand and quantify the relative degree of micromotion associated with bone defects of different sizes and different locations. This knowledge is critical to eventually understanding how any bone defects of the acetabulum can contribute to overall arthroplasty stability. Current modeling of the acetabulum is geometric only and will allow creation of a geometry based prosthesis. As this research continues reconstructions can be based on both geometry and mechanical considerations. The surgeon has a number of options when planning an acetabular reconstruction and currently the decision is based on experience. This research will lead to methodology to optimize reconstruction based on mechanical principles.

CHAPTER 2 – The Cementless Acetabular Cup

The impetus for the design of modern acetabular cups was the discovery that porous metallic surfaces held in close proximity to bone allowed the ingrowth of bone into the porous surface [4] [5]. The original acetabular cups were hemispherical porous coated cups that included a fin (Mallory Head) or a spike (AML), or a peg (PCA) to control rotation. Another design used a completely hemispherical cup with screw holes to allow the placement of screws for added stability against rotation.

The early coatings consisted of a sintered cobalt chrome, sintered cobalt chrome bead, titanium wire, or titanium plasma spray.

There have been five notable developments in cup technology. 1. Modular polyethylene liners. 2. acetabular cups were placed in underreamed fashion to create a press fit. 3. The hemispherical cup was changed to slightly oblong to create a superior peripheral "rim" fit. 4. Surface treatment of the cups has been improved to increase the coefficient of friction between the cup and the bone. 5. The development of decreased radius metal on metal monoblock cups to improve motion and decrease impingement.

The modularity of the cup has allowed for the placement of elevated rim liners so that the elevated rim could be dialed in to the proper position. When polyethylene wear has become problematic the liner could be easily exchanged with preservation of the ingrown outer cup. Early locking mechanisms allowed motion between the liner and the cup creating a second interface for the production of wear particles. Newer locking mechanisms are more robust and minimize backside wear.

Underreaming of the cup provides a tight interference fit to rigidly hold the cup until bone ingrowth occurs. Ramamurty et al in a canine study demonstrated that the degree of press fit and the bone density all played a role in determining the degree of micromotion under load [6] [7]. Underreaming of the cup of 1-2 mm has been recommended, the peripheral hoop stress that develops in the acetabulum enhances the friction creating a more rigid interface. The disadvantage of underreaming is the development of significant hoop stresses that can potentially create a fracture of the acetabulum [6] [8] [9] . A study done in our laboratory demonstrated that the hoop stresses developed with 2 mm of underreaming approached the yield strength of osteoporotic bone [10]. This risk is greater in osteoporotic bone and has been described in the literature. For this reason several authors have recommended that underreaming be limited to 1 mm.

The second disadvantage of underreaming is that a very rigid acetabulum may preclude the complete seating of the acetabular cup in the acetabulum. In very rigid bone adequate force is necessary to "bottom out" the cup.

Line to line reaming of cups required supplemental screws, pegs or fins to improve stability of the cup. The fins or pegs made placement of the cup in the exact position difficult and sometimes precluded the cup from being seated completely. The placement of screw holes necessitated the placement of screw holes in the cup itself. Screw holes and screws themselves could act as a pathway for polyethylene particles to reach the bone cup interface potentially leading to osteolysis. Consequently, there is a distinct advantage to using a full coat hemispherical cup without screw holes. Press fit fixation of the cup has been shown to be superior to line to line reaming with adjunctive fixation [11].

When a cup is unstable screw placement is critical to achieving cup stability. A single dome screw can decrease translation of the cup but can increase rotation about the screw itself [12]. Multiple screws are preferable and screws closer to the rim provide more stability than screws about the dome [11] [13].

Titanium or tantalum porous surfaces are demonstrated to have improved pullout strength as opposed to titanium plasma spray. Several manufacturers have developed highly porous high friction coatings [14].

A photoelastic bone model was loaded with different shaped implant models to understand the loading pattern of different cup geometries. trispiked, finned, hemispherical, and nonhemispherical(wider at the periphery) cups were looked at. The spiked cup generated high stresses at the point of penetration of the spikes. The fins decreased peripheral stresses. The nonhemispherial cup increased peripheral stresses more than the oversized hemispherical geometry [15].

Cementless acetabular arthroplasty relies on ingrowth of bone into a porous surface. A pore size of 50 to 400 microns is thought to be ideal for bone ingrowth. For ideal bone ingrowth, close apposition of the bone onto the metal surface, and an absence of micromotion are necessary [4]. Larger size pores > 400 microns exhibit poorer ingrowth termed macro ingrowth [4]. Micromotion between the bone and the cup can preclude the ingrowth of bone. The degree of micromotion that can preclude bony ingrowth is unknown but has been surmised to be 50 - 150 microns [16]. Pilliar et al also concluded that greater than 150 microns of micromotion could preclude bone ingrowth into a porous surface [17]. With excessive levels of micromotion

fibrous ingrowth occurs as the motion is thought to shear any incipient calcification [18] [19]. Fibrous ingrowth is not thought to be durable and may lead to eventual loosening of a cup.

A recent study evaluation the torsional stability of a cementless acetabular cup concluded that the resistance to torque was quite variable among patients and could not be adequately evaluated intraoperatively by the surgeon with current instrumentation [20].

Laboratory studies show in an animal model that in a well fixed cup that becomes ingrown, the ingrowth of bone is associated with a decrease in micromotion at the cup bone interface [21]. A study in sheep of a cup coated with Sulmesh demonstrated that adequate fixation of a cementless cup was provided by implantation of a relative oversized cup into an acetabulum [22]. The authors noted that the cup stability to a torque increased three fold with bone ingrowth into the cup.

A study of various designs of porous acetabular cups showed that cup subsidence increased between 500 and 10,000 cycles and with 300 kg loads micromotion increased over 150 microns in most cups [23].

A dog study of cementless acetabular cups showed the percentage of ingrowth at 6 months to 12%. This increased to 24% both at 12 and 24 months [24].

Retrieval studies of Cook et al showed lower rates of bone ingrowth than other studies [25]. In a retrieval of 42 acetabular cups ingrowth was noted in 28 of 42. Bone ingrowth occurred more frequently, in greater amounts and was more evenly distributed anatomically in cups using screws for initial adjunct fixation. Roentgenographic and clinical findings were unreliable in predicting ingrowth of bone.

A more recent study of porous tantalum cups in dogs showed that bone ingrowth averaged 25.1% [26]. The authors found that the greatest ingrowth was peripherally where bone prosthesis contact was most consistent.

In a retrieval study of 25 porous coated titanium acetabular components implanted with secondary screw fixation, Sumner et al showed that 18/25 showed ingrowth with up to 1/3 of the void space within the porous coating occupied by bone [27]. The maximal proportion area occupied was over 80%. Bone ingrowth was more often observed at the dome and in the vicinity of screw fixation.

Another study by the same group showed the average volume fraction to be 12.1 (8.2%) [28]. Bone ingrowth is particularly in the area of the dome and in the vicinity of sites of screw fixation. Bone ingrowth peripherally was less consistent. Autopsy retrievals from the Anderson Orthopaedic Institute showed unpredictable growth in the acetabular component ranging from 3% -84% and averaging 32% [29].

Nishii et al found no correlation between osteoblastic response to arthritis in the hip and the outcome of cementless fixation [30].

The aim of cementless fixation of a porous coated cup is to maintain the porous coating of the cup in close apposition to the acetabular bone permitting ingrowth of the bone into the porous coating. For this process to occur two things are necessary 1: close apposition of the cup to the bone, 2 minimal motion between the bone and the coating. Motion greater than 150 microns will preclude bony ingrowth and can lead to fibrous ingrowth of the cup. Fibrous ingrowth may not be durable and can lead to pain or eventual loosening of the cup.

Line to line placement of a cup allows almost complete contact between the bone surface and the bone. However line to line placement is relatively unstable as torque on the cup due to impingement or microseperation and eccentric loading may produce a torque at the interface creating unacceptable micromotion. When line to line placement is performed, screw fixation of the cup is necessary.

Won et. al. also looked at the effect of screw fixation [9]. They noted that adding screws decreased the micromotion at the site of the screw but increased motion at the opposite side of the cup. Screw fixation can also create neurovascular injury [31]. When line to line fixation is contemplated is necessary to use a cup with screw holes for screw placement.

The primary fixation of a porous cementless cup is through undersizing of reamed acetabuluum producing an interference fit. Hoop stresses are created in the acetabular rim creating a normal frictional force at the cup bone interface.

Won et. al. looked at line to line vs underreaming of a porous acetabular cup. They noted that excellent fixation could be achieved with underreaming of 2-3 mm [11]. Underreaming greater than 2 mm however can be associated with increased hoop stresses that can cause fracture upon insertion [10].

CHAPTER 3 – Etiology Location and Classification of the Deficient Acetabulum

Defects of the acetabulum can occur from developmental problems associated with congenital subluxation or dislocation [32]. Frequently the congenital dislocated hip will show inadequate coverage of the femoral head with a shallow acetabulum. The bone column may not be thick enough to obtain adequate coverage of the cup.

Fractures of the acetabulum especially those that have not undergone open reduction and internal fixation can show significant bone deficiency [33] [34] [35]. Ununited fracture fragments of the posterior or anterior wall are unable to support a cementless cup.

The most frequent cause of bone loss and bone defects is osteolysis. The modern total hip arthroplasty consists of metal stem and articulating ball as well as an acetabular outer shell with an inner polyethylene insert. The metal ball of the femoral component articulates with the polyethylene liner. Frictional wear between the femoral head and liner creates wear particles which are submicron and are extremely biologically active. Osteolysis and bone loss occurs as a reaction to wear particles [36] [37] [38]. A total hip arthroplasty that has been present for several decades will create substantial volumetric wear in the form of submicron particles. This can lead to cup loosening as well as significant structural bone loss.

The acetabulum is composed of the confluence of three bones, the ischium, the illium and the pubis. The acetabulum is shaped as an inverted V visible from inside the pelvis. The base of the V is the obturator foramen. The anterior and posterior limbs of the inverted V are the anterior and posterior columns, which are regarded as critical for stability of the acetabulum. Visualizing the acetabulum from the lateral side of the body the acetabulum is a curved inverted crescent moon shaped surface termed the lunate surface that articulates with the femoral head. The lunate

surface surrounds the acetabular fossa. The inferior portion of the acetabular fossa is termed the acetabular notch. The acetabular notch opens into the obturator foramen inferiorly (Figure 1).

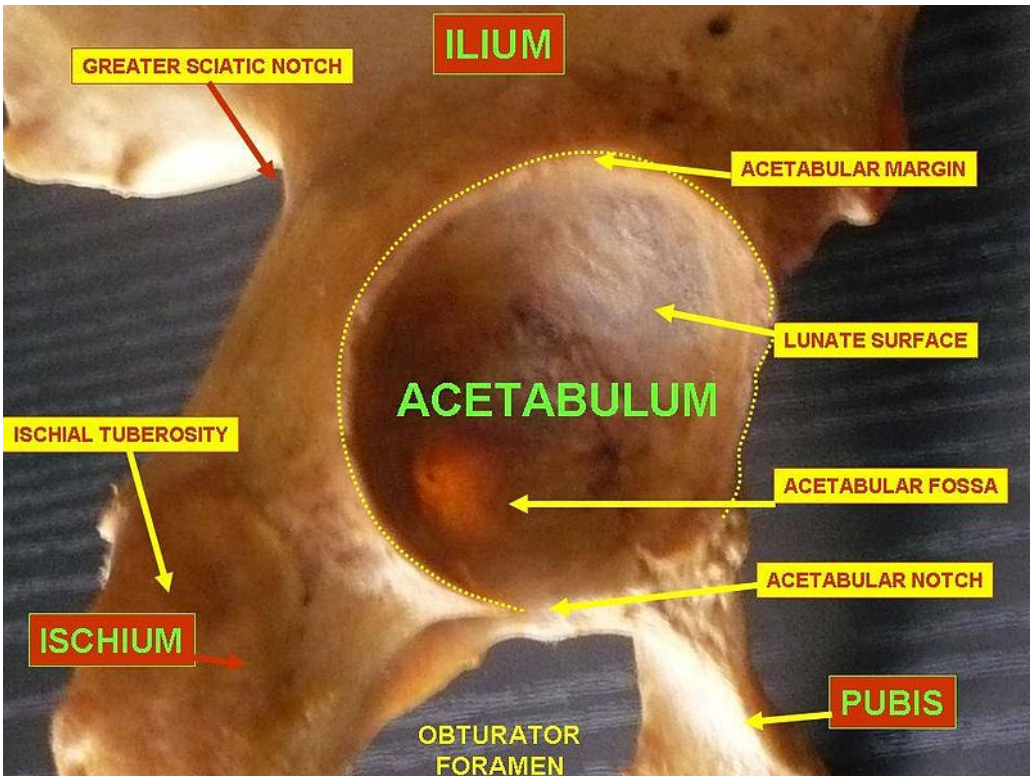

Figure 1 - Anatomy of the Acetabulum - Lateral View -The three bones constituting the acetabulum the ilium, the ischium and the pubis are illustrated. (Creative Commons: Wikipedia)

The acetabular columns are key to the stability of the cementless acetabular cup. Fractures or defects in a column of the acetabulum preclude fixation of the acetabular cup.

When reconstructing the acetabulum after failure due to osteolysis, cup stability may be threatened by bone loss. The second critical factor is that bone loss may adversely impact osseointegration potential through decreased bone-implant contact area [39].

Classification systems for bone deficiency currently in use are the Paprosky and the AAOS system [40] [41] [42]. Both systems are descriptive in nature but neither evaluates the mechanical stability of the deficient acetabulum and its effect on cup stability.

Paprosky developed the classification evaluating 147 patients. The four criteria used to assess the preoperative radiograph are 1. Superior migration of the hip center, 2. ischia osteolysis, 3. Teardrop osteolysis, and 4. Position of the implant in relation to Kohler's Line (Table I) [43]. Superior migration indicates loss in the dome involving the anterior and posterior columns. Medial word migration has preferential loss of the anterior column and lateral migration shows preferential loss of the posterior column. Ischial osteolysis indicates loss of the inferior aspect of the posterior column, while teardrop osteolysis indicates loss of the medial and inferior aspects of the acetabulum. In Type 1 there is minimal loss of the rim and walls and reconstruction can be done with a cementless cup. In type 2 the acetabular rim and walls are distorted, but there is adequate bone for support of a cementless prosthesis. Type 2a: Superior migration with the superior rim intact, Type 2b superior acetabular rim is missing, Type 2c medial wall defect with migration medial to Koehler's line. Type 3 defects have compromise of the walls and rim. Migration is greater than 2cm proximally. Type 3a involves more than 1/3 but less than ½ of the acetabular rim. There may be adequate bone for ingrowth but structural augmentation is necessary for initial cup fixation. Type 3b involves more than half of the circumference.

Acetabular defects were graded pre-operatively on a plain AP radiographs. Intra-operatively 11% of grade II defects were upgraded to type III and 5% of type III defects were downgraded to type II. The intra- and inter-observer reliability of the Paprosky classification of plain radiographs have been found to be moderate to poor by other authors [44] [45] [46].

Table 1 - The Paprosky Classification of Acetabular Defects

Type	Description
Type 1	- Rim is intact w/ no significant distortion of the rim - Acetabulum is hemispherical but there may be small focal areas of contained - Anterior and posterior columns are intact
Type 2	- Distorted but intact rim with adequate remaining bone to support a hemispherical cementless implant.
Type 2A	- Anterior and posterior columns are supportive and the rim is intact bone loss is superior and medial.
Type 2B	- Superior rim is deficient for less than one third of the rim circumference; - Migration is less than 3 cm above the obturator line directly superior or in combination with lateral migration.
Type 2C	- There is medial wall defects and migration of the component medial to Kohler's Line - Rim of the acetabulum is intact and will support the component
Type 3	- Acetabular rim is not adequate for initial stability of the component
Type 3A	- Characterized by greater than 3 cm of superior migration of the femoral component cephalad to the superior obturator line. - Moderate teardrop and ischial lysis, and an intact Kohler line.
Type 3B	- There is less than 40% of host bone available for ingrowth - Rim defect is greater than 1/2 circumference

Table 2 - AAOS Classification of Acetabular Defects

Type	Description
Type I Segmental Deficiency	
A	Peripheral: Superior/ Anterior/Posterior
B	Central Medial Wall Absent
Type II Cavitary Deficiency	
A	Peripheral: Superior/ Anterior/Posterior
B	Central Medial Wall Absent
Type III	Combined Segmental and Cavitary Deficiency
Type IV	Pelvic Discontinuity
Type V	Arthrodesis

The American Academy of Orthopaedic Surgeons (AAOS) classification distinguishes between segmental and cavitary defects (Table 2) [42]. Type I are segmental defects that are peripheral (IA), involving superior, anterior or posterior rim, or central (IB) with absent medial wall. Cavitary defects or volumetric expansions are classified as type II and sub-classified once again into peripheral (IIA) and central (IIB). Combined segmental and cavitary defects are classified as type III, pelvic discontinuity type IV and arthrodesis type V. This is a descriptive classification that does not provide the surgeon with a guide for reconstruction options. Poor reliability has also been demonstrated with this classification system.

Mechanically the validity of the Paprosky Clasification has been questioned because it does not accurately predict the degree of bone loss that can influence the degree of cup stability [44] [45] [46]. Both classifications are descriptive in nature but either is based on mechanical stability.

The current project endeavors to understand the mechanical effect of bone defects on cup stability. We believe that mathematical modeling will prove superior to a descriptive classification in planning and optimizing a construct to rebuild an acetabulum with structural bone loss.

CHAPTER 4 – Current Treatment and Solutions for Patients with a Defective Rim

Currently the cementless acetabular cup provides excellent fixation in an arthritic acetabulum without bone loss. As described in previous chapters, an intact rim is necessary for a durable and stable press fit fixation. Small defects in the rim may have little defects but larger defects can decrease the rigidity of the cementless cup as placement of an underreamed cup will not create hoop stresses or a frictional compressive force to stabilize the acetabular cup.

The stability and fixation can be compromised due to deficiencies on the posterior or anterior acetabular walls [43]. The integrity of the acetabular wall is important for cup fixation and stability because defects often result in a lack of fixation at the cup-bone interface due to uneven contact at the interface [23]. A number of corrective methods for stabilizing the wall prior to cup implantation are currently in use, such as bone grafting [47], screw fixation [13] [48] or the use of metal augments [49] [50] [51].

Well-fixed components that demonstrate osteolysis of the acetabulum associated with polyethylene wear can be treated with bone grafting of the defects and replacement of the worn polyethylene liner [52] [53]. In cases of superior migration with an intact rim, a cementless cup can be placed superiorly or the ovally deformed cup can be overreamed to a large diameter for a "jumbo' cup [54] [55] [56]. Another option is the bilobed cup that has an oval shape [57] [58]. The placement of metallic wedges can also be used to fill a superior defect (Figure 2) [49] [50] [51].

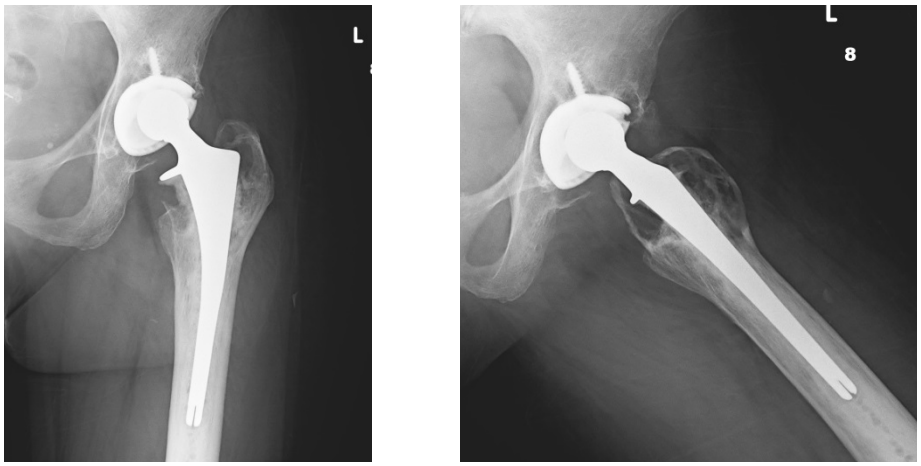

Figure 2 - Cementless Cup showing osteolysis about the stem and cup with eccentric position of the femoral head due to polyethylene wear.

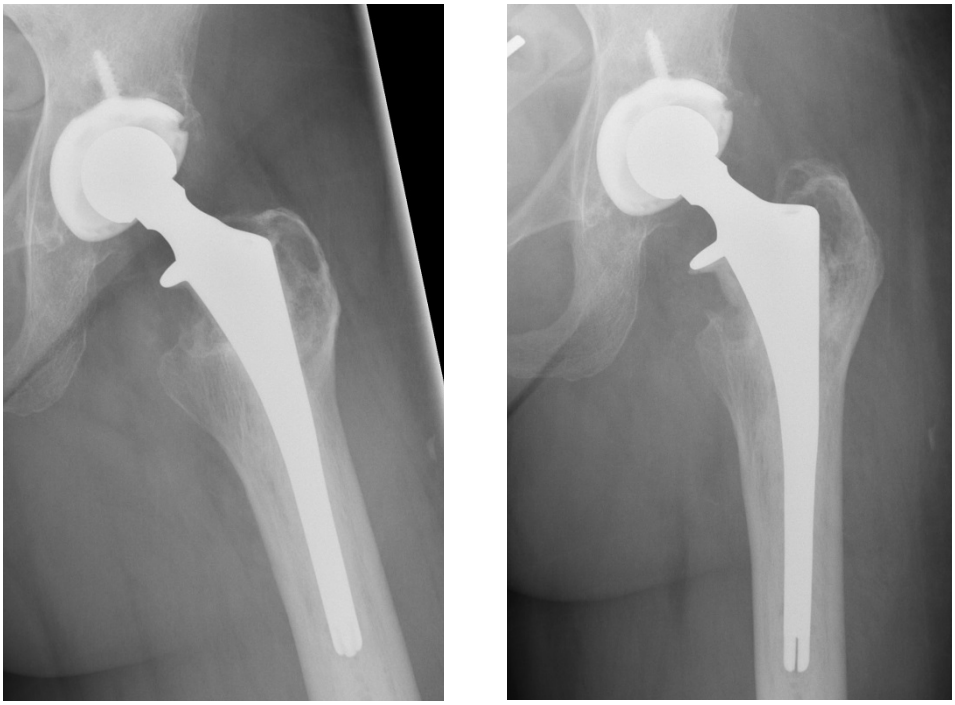

Figure 3 - Cup after bone grafting and liner exchange showing well centered prosthetic head in cup. Osteolytic defects have been grafted.

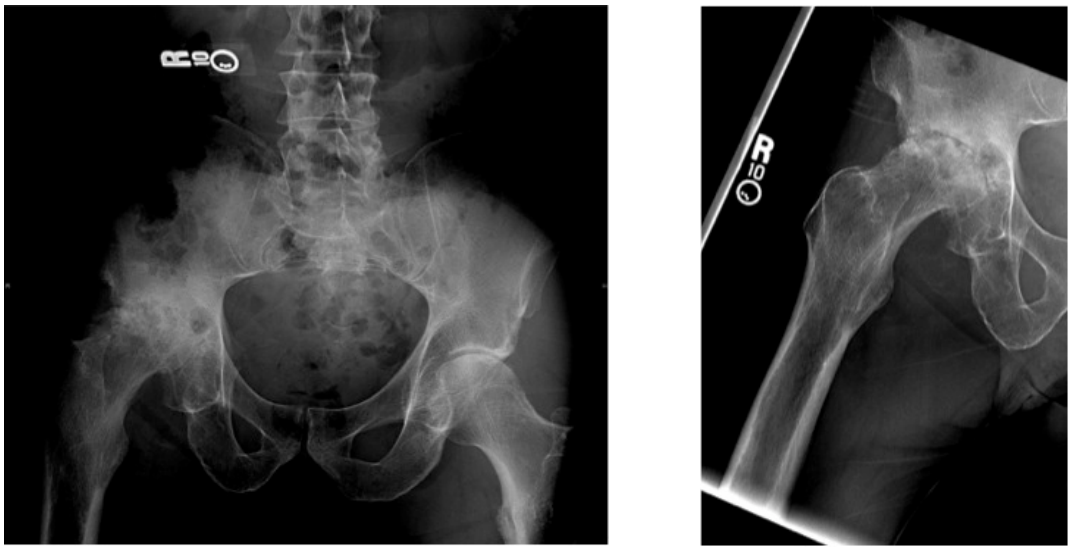

Figure 4 - Arthritic hip with superior migration of the femoral head. There is significant superior bone loss, loss of joint space and loss of sphericity of the femoral head.

Figure 5 - Hip Arthroplasty with superior metal wedge placed above cup to reconstruct superior defect. The superior migration of the femoral head is corrected with the head in an anatomic position.

More severe bone loss may preclude the fixation of a simple cementless hemispherical cup. In this case there are several options. The cemented cage construct has shown poor long term survival. The "trampoline" a trabecular metal revision shell is a metal cage like construct

fits into a cementless cup [59]. The cup is off loaded and stabilized by the cage until bone ingrowth. The final option is the use of a custom made cup with porous coated flanges [60]. A CT scan is used to create a solid model and from the model a custom cup with porous coated flanges. (Figure 6 - Figure 9)

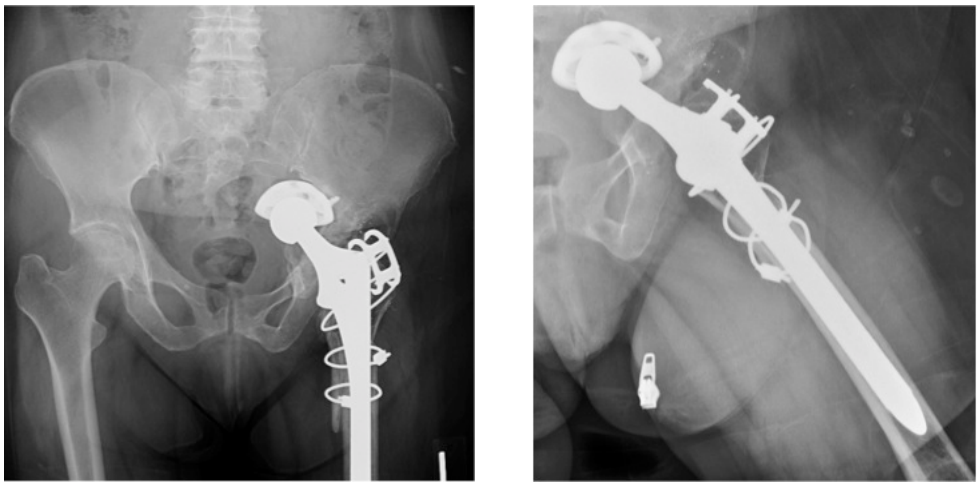

Figure 6 - Failed Hip Arthroplasty with migration of the cup into the pelvis. There is complete obliteration of the medial wall of the acetabulum.

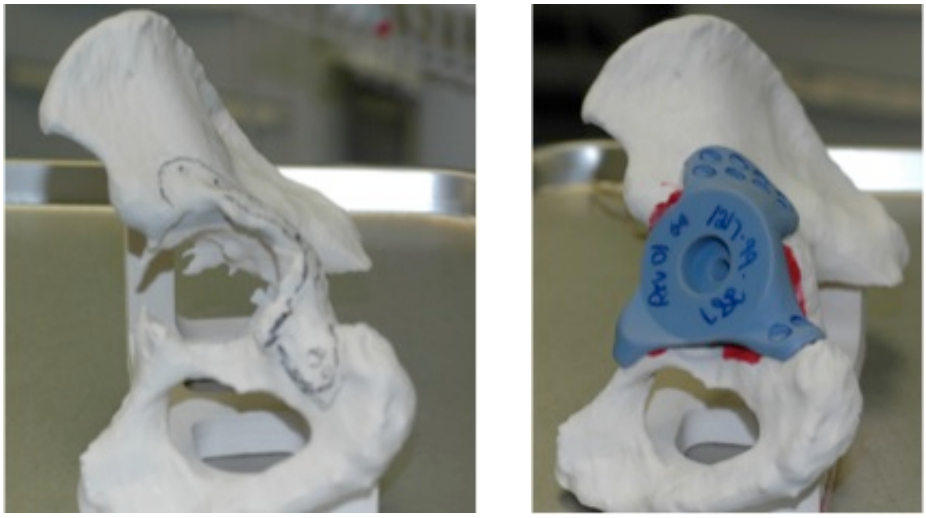

Figure 7 - Acetabular Model and model of custom designed cup, made from CT scan of deficient acetabulum. Flanges are designed to anchor to the ilium and ischium with screws.

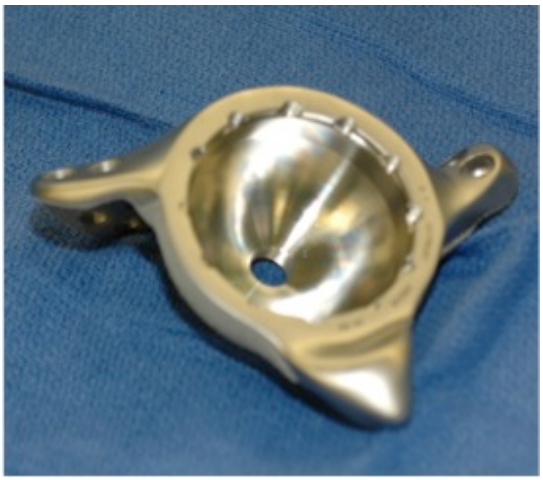

Figure 8 - Custom designed cup with porous coated flanges.

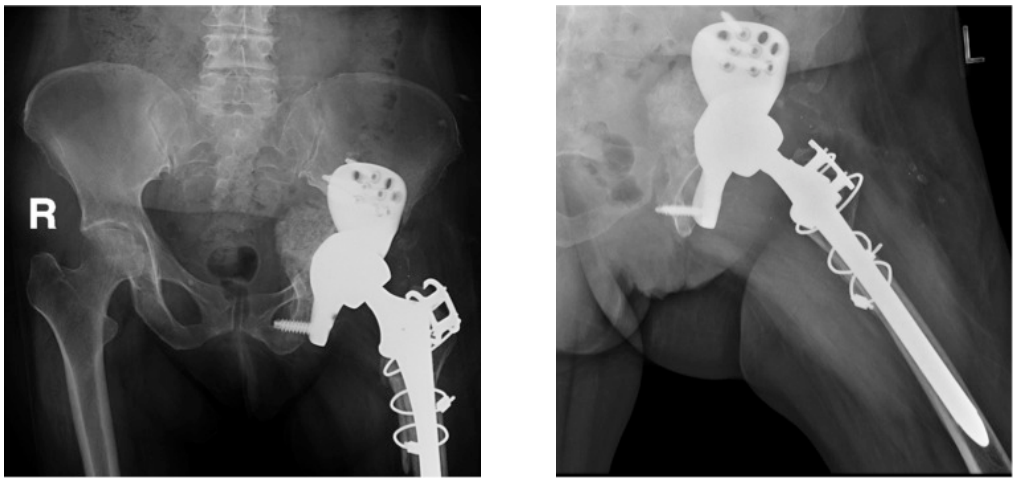

Figure 9 - Reconstruction of acetabulum with custom designed cup. Note screws anchoring the cup into the illium and ischium. Femoral head is in the near anatomic position.

Bone grafting can be utilized to fill bone defects caused by osteolysis. Structural bone grafts are not recommended. As bone graft becomes revascularized the bone can lose its initial mechanical properties and allow collapse of the construct [61] [62] [63]. Bone substitutes have also been used to reconstruct defects in a nonstructural application.

The Paprosky and AAOS classifications are descriptive and are not based on mechanical principles. We hypothesize that the size and position of a rim defect about the acetabulum both are variables that determine the degree of stability of a pressed fit acetabular cup. To better understand the mechanical stability of a cup in the face of bone defects.

CHAPTER 5 – Experimental Methods and Loading of the Cup

The experimental methods make use of position micro-sensors used to measure the cup bone interface after a THR in cadaveric specimens. The experiment consisted of manually creating a precision defect, implanting acetabular cups though the same procedure used in patients including under reaming, cup positioning and insertion of the cup. The second phase focused on instrumenting and load testing the hemipelvises using a specially designed fixture and Instron machine. The data acquisition and its methodology are based on previous works performed in the Biomechanics Research Laboratory [10] [64] [65]. The workflow of the experimental method is diagramed in Figure 10.

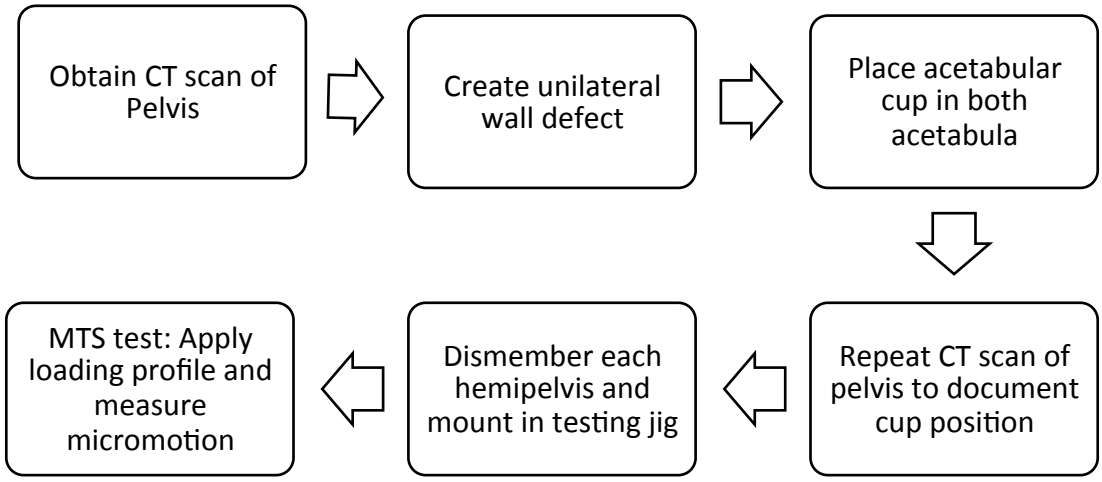

Figure 10 - Workflow of experiment.

Defect Creation

Each of the two pelvises was removed from a fresh-frozen cadaver, which was previously maintained at -20°F. The pelvises were free of any musculoskeletal or structural abnormalities as

noted on visual inspection. After thawing the pelvises, they were imaged with CT scan prior to disturbing any pelvic tissues.

Next, the pelvises were dissected using a postero-lateral approach to expose the acetabulum, and the femur was dislocated. The labrum and all soft tissue in the fovea were removed. Following the methods described above the appropriate defect location was identified and outlined on the specimen. A rongeur, osteotome, and mallet were used to create the full-thickness defect. (Figure 11) A Vernier caliper and ruler were used continuously throughout the procedure to confirm that the defect size was correct. Following defect creation, a second CT scan was performed on the pelvis.

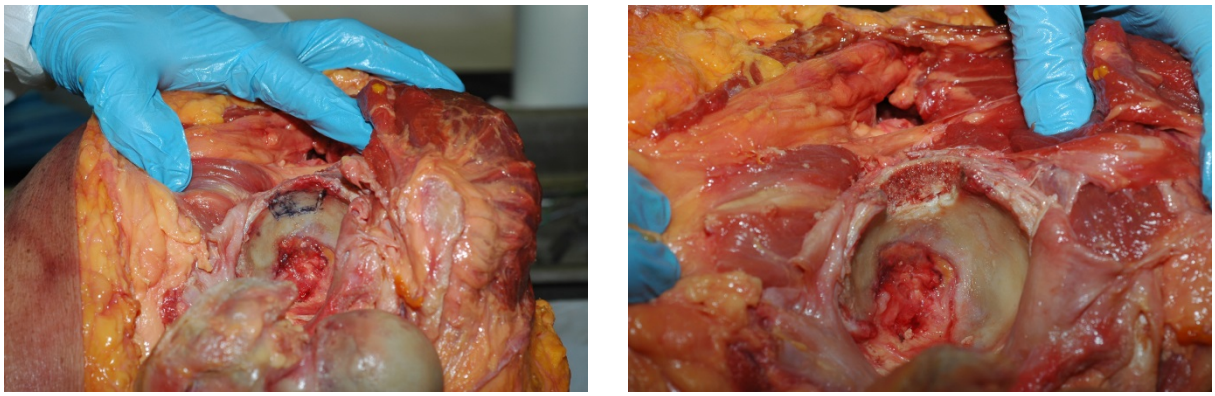

Figure 11 - Creation of superior acetabular defect. Chisels are used to create the defect.

Cup Implantation and THR procedures

Two full sets of Johnson & Johnson Gription implants (ranging from 54mm to 66mm), along with the necessary surgical instruments, were available before starting the cup implantation procedure. The procedure began by fully removing the femur, as it was not needed. Reaming proceeded by increasing in 1mm diameter increments until an appropriate final diameter was reached, using the same criteria as would be used during an actual procedure. The

criteria to determine how much to ream was the same as used in surgery, and included: maintaining the anterior, posterior, and medial wall, while removing all hyaline cartilage such that an exposed bed of bleeding bone was visualized. Given that the tissue was not living, an estimate was made as to when a bed of bleeding subchondral or cancellous bone would occur. The Gription cups were implanted with 1mm of under-reaming. The cups were impacted with a mallet at 45° of inclination and 30° of anteversion. The medial wall of the pelvis was visualized through the apical hole of the cup to ensure the cup was fully seated. The same surgeon (MHG) performed both implantations.

After defect creation and cup implantation, the pelvises were hemi-sectioned through the pubic symphysis and sacrum with all soft tissues still in place. The soft tissues help dampen the vibration of the bone saw and minimize any potential damage to the pelvis created by the bone saw vibration. The pelvises were then denuded of all soft tissues and potted (using Bondo®) in a structural metal box. Importantly, the cup rim was carefully maintained in the horizontal plane as the cement cured. Also, a line on the pelvis between the ASIS and ischial tuberosity was maintained parallel to the side of the metal box. These two preceding criteria define the reference system described below (see Figure 14). A third CT scan was performed of the potted pelvises with cups implanted for use in separate analysis.

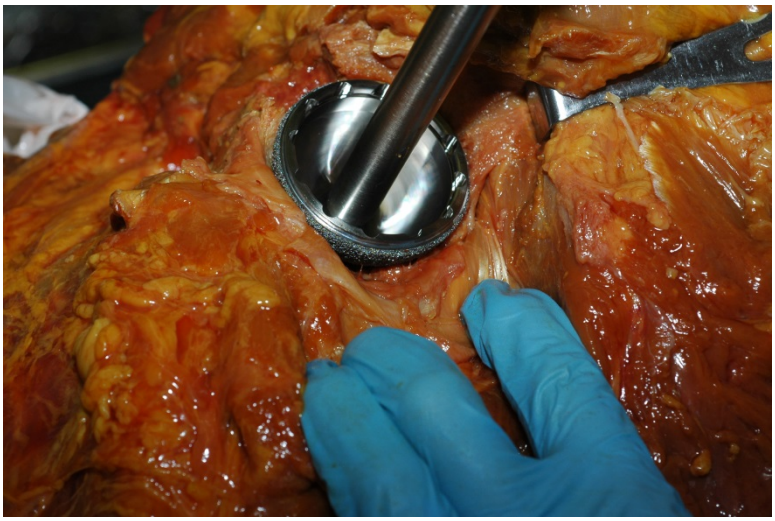

Figure 12 - Placement of acetabular cup. The acetabulum has been reamed and the cup is impacted into the acetabulum.

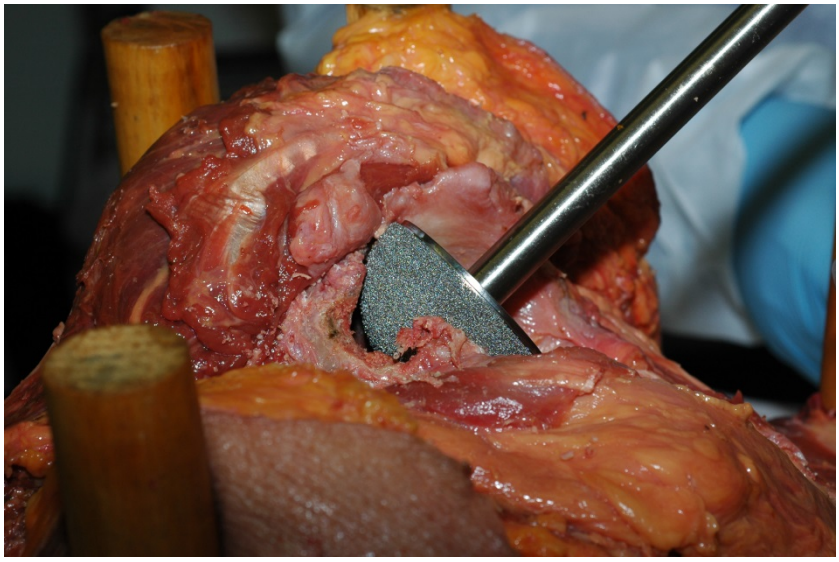

Figure 13 - Placement of acetabular cup showing superior defect. The cup is being impacted. The portion of the cup uncovered by the defect is visualized.

CHAPTER 6 – Instrumentation, Sensor Placement, Data Acquisition and Load Profile

Reference Frame and Coordinate Systems

The cubical structural metal box that the pelvi are cemented in is used to define a 3-D axis coordinate system (Figure 14). A line drawn through the ASIS and ischial tuberosity is maintained parallel to the side of the metal box as the cement cures. Additionally, the rim of the acetabular cup is maintained in a horizontal plane, parallel to the bottom of the box. This coordinate system is used in several other studies (Figure 15, Figure 16) [48]. Lee, et.al. visually divided the acetabulum into 4 quadrants intraoperatively and estimated the percentage of bone not in contact with a trial acetabular cup (Figure 16) [62]. They then used these numbers to determine the percentage of the cup in contact with the bone, and therefore the defect size. Other coordinate systems include orienting the boney acetabular rim in the horizontal plane, with a centerline through the center of the acetabular notch.

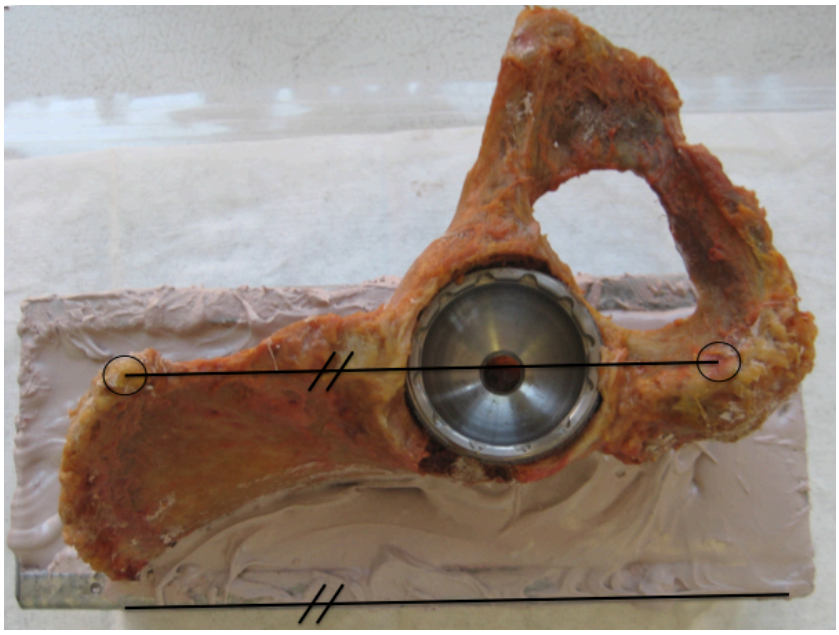

Figure 14 - Coordinate system. The longitudinal axis runs from the anterior superior iliac spine to the center of the ischium.

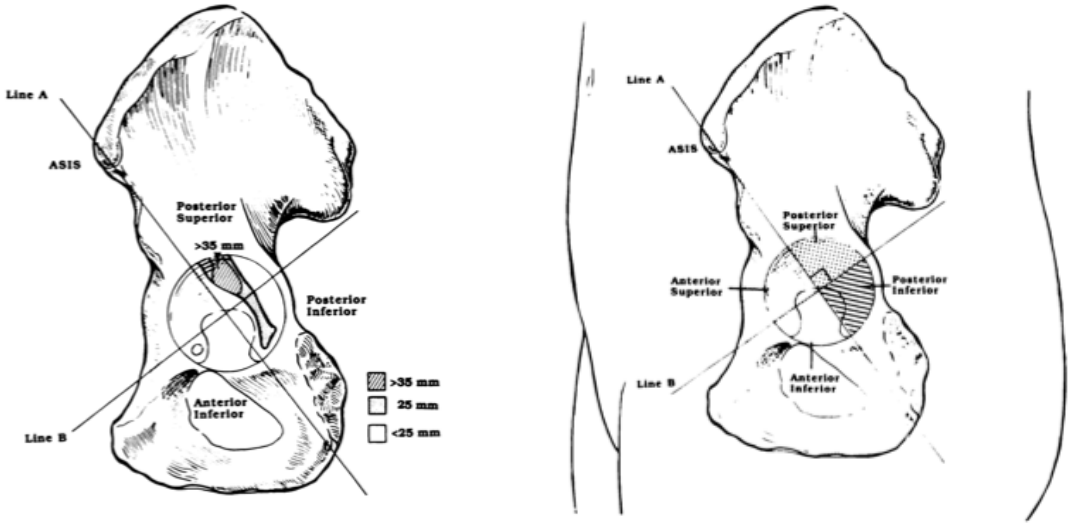

Figure 15 - Coordinate System Quadrants Illustrated. The longitudinal axis from the anterior iliac spine to the center of the ischium is shown. The second axis is perpendicular to this bisecting the acetabulum.

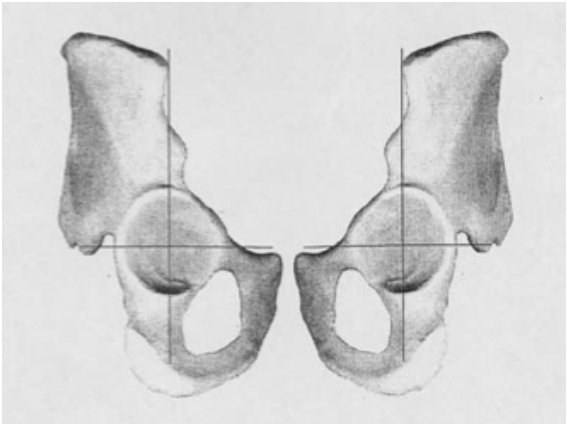

Figure 16 - Quadrant Position in relation to Pelvis. The axis of the pelvis in an upright position is illustrated.

Instrumentation and Sensor Placement Description

Each hemipelvis and acetabular cup was instrumented with eight linear variable differential transducers (LVDT, Trans-Tek Inc., AC-DC 332). LVDTs are capable of measuring the small displacements that a pelvis and acetabular cup experiences under loading conditions (e.g., during walking, jogging, squatting, etc.). The resolution of each LVDT is 20um (≈0.00079 in). The support and adjustment structures surrounding each LVDT are relatively large, and therefore a unique support scaffold was built and is described below (Figure 17).

A 0.500" diameter metal rod was rigidly attached to the apical hole of the cup in a vertical orientation. A metal "cross" was attached to the vertical rod and used as the LVDT contact point to capture cup motion. A total of six LVDTs contacted the metal cross. Three were along the Z-axis (#1-3 in Figure 18) and three were radially out from the center of the metal cross (#4-6 in Figure 18). Lastly, two LVDTs contacted the boney rim of the acetabulum along the X and Y-axis to capture acetabular cup expansion under loading (#7-8 in Figure 18). It is

assumed that no rotation around the Z-axis takes place. The combination of LVDTs #1-5 allows a kinematic analysis of the five degree of freedom acetabular cup (Figure 19).

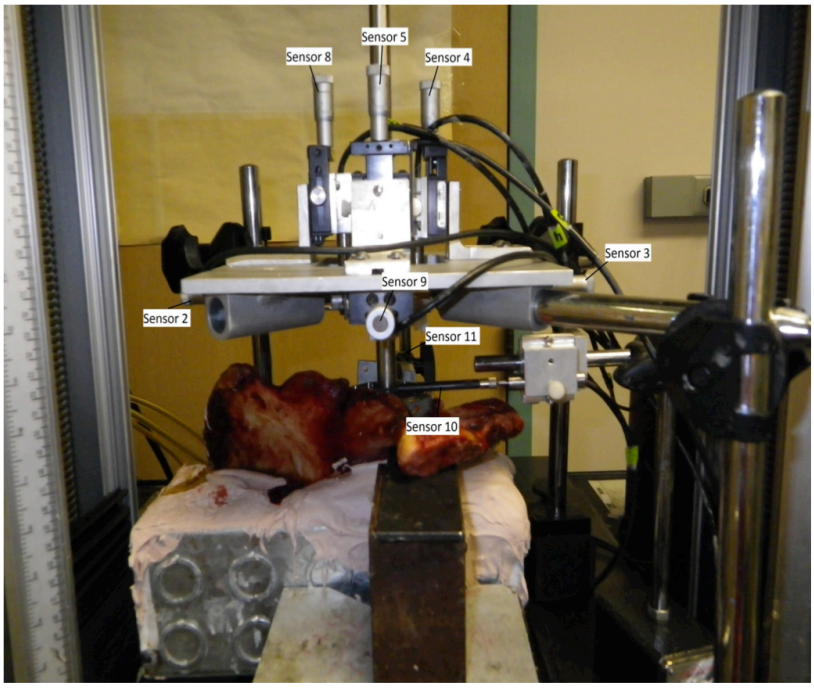

Figure 17 - Experimental Setup showing position of sensors. The key sensors used are the superior posterior and anterior sensors.

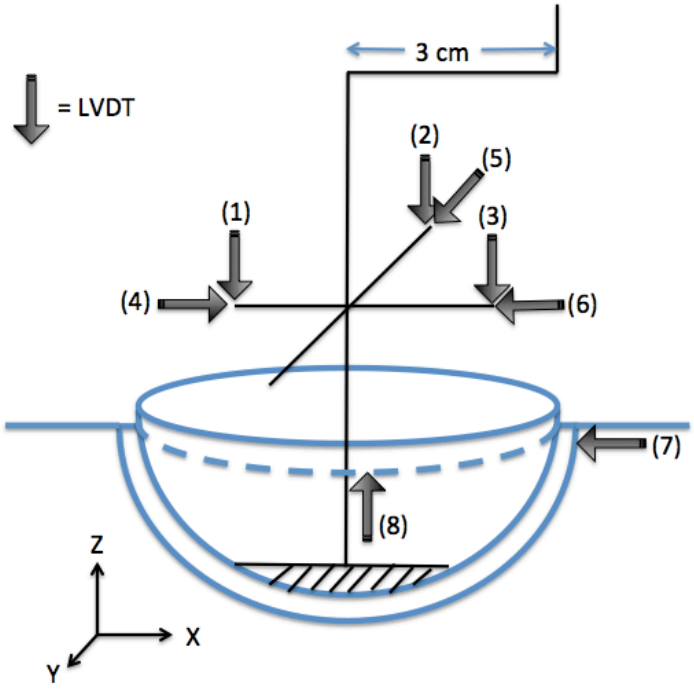

Figure 18 - LVDT placement diagram for Testing of the cup-bone interface.

Description of Load

An offset compression load was applied along the Z-axis through a metal rod which was rigidly attached to the apical hole of the acetabular cup (Figure 19). An Instron® Static Hydraulic Loader applied the load, and the load was offset 18mm along the X-axis in the direction of the ischial tuberosity.

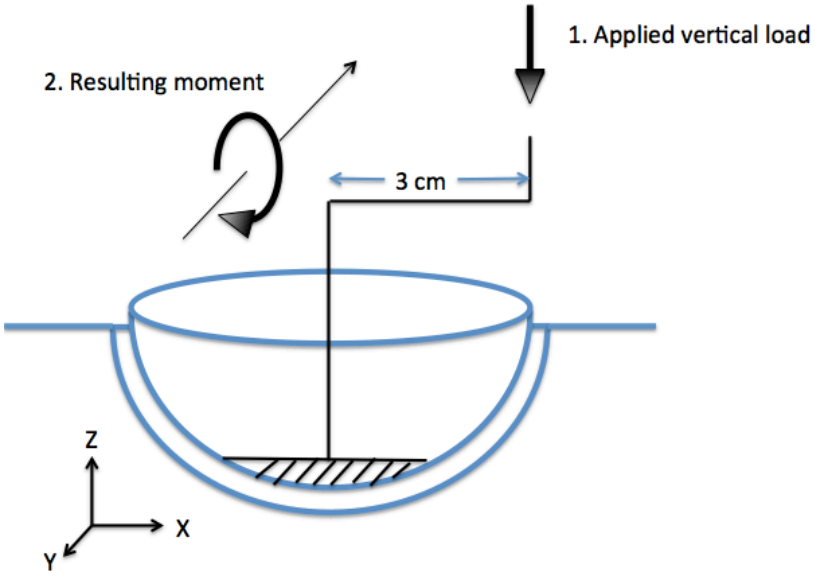

Figure 19 - Schematic of applied torque and normal force to acetabular cup.

Load Profile

The applied load began at zero and increased to the set maximum load, at a linear ram velocity of 2 mm/min. Once the maximum load was reached, the ram returned to 10N of load (defined as zero load) at 2 mm/min. This load-unload cycle was repeated three times for each maximum load setting. The maximum load setting ranged from 25-1500N in increments of 25N for a maximum load of 25-300N (i.e., a maximum of 25, 50, 75, etc.), and in increments of 50N for 300-1500N (i.e., a maximum of 300, 350, 400, etc.). The moment arm generated a maximum torque that ranged from 0.45-27 N-m.

The load profile applied to the acetabular cup was chosen to simulate a combination of the greatest forces experienced by a THA patient during walking and subluxation. The peak normal force applied (compression component) simulates a brisk walk or jog, whereas the peak torque applied (moment component) simulates subluxation potentially experienced while rising from a chair or squatting position. The hip reaction force can vary from 3-5 times body weight in

single leg stance and during ambulation for the native hip [66]. The peak compressive load after total joint arthroplasty has been shown to be slightly diminished over the native hip because of a decrease in cadence [67]. For reference, the peak normal force of 1500N used in this study is equivalent to statically supporting 337 lb., on one hip joint. Four times body weight for a 175 pound man is 3115 Newtons.

At the extremes of motion a total hip arthroplasty can impinge or sublux and relocate. Both conditions load the joint eccentrically producing a torque on the interface. For this reason the load is applied with an offset to also apply a torque to the interface [68].

Directly comparing acetabuli on the same pelvis allows the experiment to control for several potentially confounding variables (e.g., cancellous bone density, cortical bone thickness, resultant coefficient of friction of the reamed acetabular surface, etc.). Although some differences may exist between the right and left side of the same pelvis, this is the most practical method to mitigate these potential differences.

Data Acquisition

Two different software programs were used to collect data. The Instron® software managed ram position and recorded applied load using a built-in 50 kN strain gauge, as a function of ram position. Separately, LabView collected LVDT position data, as a function of time. These two sets of data were later combined into one set by matching peak values in the separate position-based and time-based data sets.

Repositioning of sensors proved to be one challenge in data acquisition. Each sensor has a total measurement range of approximately 2mm. However, this is reduced to about 1mm since testing begins with each sensor in the middle of its measurement range. The total travel range

required of each LVDT during the experiment is greater than 4mm; thus, repositioning is required. Recording LVDT position during adjustment (for use later as a "calibration") solves this problem. The recorded start and end position of the LVDT in the calibration file allows the pre- and post-adjustment data to be aligned later, during the data analysis phase.

CHAPTER 7 – Development of the Model

The cementless cup is commonly placed in an acetabular cup that has a diameter 1 mm smaller than the cup. The cup has a porous roughened outer surface that has been described previously. The cup is shaped as an inverted U with a defect inferiorly.

When the cup is placed the acetabulum is forced to enlarge. There is a combination of plastic and elastic deformation. The literature documents local crushing of the trabecular associated with cup insertion. Once a cup is placed changing position is known surgically to decrease the stability of the cup.

Initially cup placement was modeled with the bone as a purely elastic material and the cup as a completely rigid material. The cup was "impacted" into the underreamed acetabulum by forcing the dome of the cup into contact with the dome of the acetabulum. As soon as the initial constraint was released the cup "snapped back" maintaining equatorial contact only. We believe that hoop stresses created friction in this model that held the cup in place at the equator only (Figure 20).

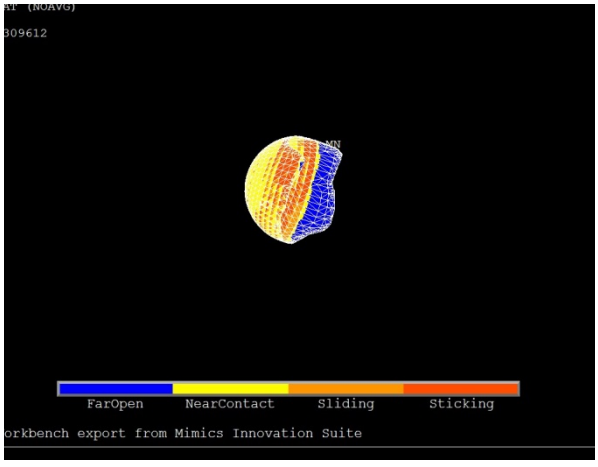

Figure 20 - Model of a purely elastic bone cup interface showing contact (red) only in the equatorial region. Note near contact (yellow) at the dome of the cup.

This model of purely elastic deformation of the bone was abandoned because we believed it did not accurately represent the experimental interface. Convergence of the model as the bone deformed could not be achieved reproducibly. We believe that the experimental cup created plastic deformation at the rim, but there is an element of elasticity that causes the cup to snap back so that dome contact is not present.

Clinically it is obvious that the interface is not purely elastic. When a cementless cup is placed and the position changed the interface is degraded and the cup becomes unstable. The acetabulum must be reamed once again and the cup reimpacted to create a new interface.

It has been shown in a canine study shown that primary fixation of a cementless cup is much greater about the equator [26]. Retrieval studies have shown ingrowth about the rim and and about screws in the acetabulum [28].

It was decided to bind the cup to the rim of the inverted U in an arc covering 270 degrees. The bonded contact is created in an equatorial rim accounting for 15-25% of the overall surface area of the cup.

The first experiments evaluate the effect of decreasing the width of the constrained surface at the equator of the cup. This was specifically conducted to evaluate two new designs of the cup. The Durom (Zimmer) and ASR (Depuy) cups both showed a decreased radius of 165 to 170 degrees (less than the 180 degree full hemispherical cup). This was done specifically to reduce impingement of the femoral neck on the cup. However in so doing the equatorial area of contact is diminished.

Clinical reports showed that a relatively high percentage of these decreased radius cups were failing within the first six months of their implantation. Although there are problems noted

from wear in metal on metal cups, this problem manifests itself in later formation of Aseptic lymphocytic lesions (ALVAL) [69]. The time course of the ALVAL lesion is several years. The early cup failures were as a result of bone failing to ingrow [70] [71] [72] [73] [74] [75]. This points to initial fixation as being a problem. The question is can a decreased equatorial region and decreased equatorial fixation lead to increased micromotion and failure of ingrowth.

The second scenario was conducted to evaluate the dual radius cup. Several manufacturers have designed a cup with a larger radius at the equator than at the dome. This was designed to improve compressive forces at the equator. Practically by decreasing the radius of the dome contact on the dome side of the equator is also diminished. This has been modeled by decreasing the width of the equatorial constrained band on the inner side.

The second experiment evaluates the effect of bone defects on cup stability. Bone defects are created at 45 degree intervals and involve 17-23% of the constrained equatorial nodes. The difference in position has two important factors. First the inferior defects will outside the two structural columns and may have less effect on micromotion than a defect in a structural column. Secondly, since the equatorial area of constraint is the upper 270 degrees of the arc, a defect not bridged by the constrained nodes may have more micromotion than defects bridged by constrained nodes.

The third experiment evaluates micromotion as a function of defect size. Three defect sizes were evaluated at two positions the seventh and second position. The positions were selected because the second position is bridged by the constrained nodes and the seventh position is not bridged by the constrained nodes.

CHAPTER 8 – Computer Modeling of the Acetabulum Based on CT Data Using CAD/MIMICS

The right hip of the cadaver is exposed and a 1 X 2 cm defect is created in the acetabulum in the posterolateral aspect of the acetabulum. (see CHAPTER 7 – Development of the Model). A CT scan is obtained of the pelvis and the frame of reference is termed the "Body" Frame of reference. The acetabula are each reamed and an acetabular cup is placed in each.). After cup placement each hemipelvis is dissected from the body and potted into a metal holder or "Box". After potting, a CT scan is obtained of each potted hemipelvis. Each hemipelvis in the "box" is then loaded with a prescribed torque and compressive force and the micromotion is measured.

To create the model a solid model of the pelvis is constructed from the CT scan (Dicom) image of the pelvis. The workflow of the modeling process is shown in Figure 21.

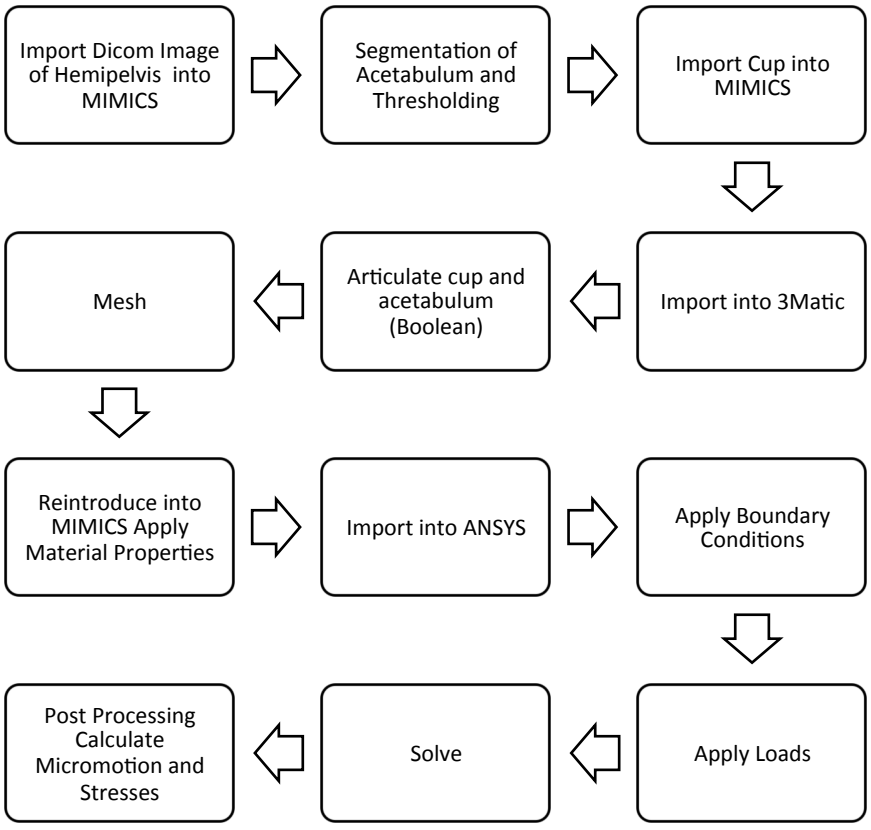

Figure 21 - Workflow of Model Creation

The Dicom Images are imported into MIMICS. The images are segmented using a bone threshold to create a mask containing the bony pelvis and sacrum only while excluding all soft tissue. Manual segmentation followed by region growing is then performed to isolate each hemipelvis. A mask is created of each hemipelvis isolating it from the contralateral hemipelvis and sacrum. The right hemipelvis contains the defect and the left hemipelvis is pristine. Both hemipelvis' are in the "Body" frame of reference.

Each hemipelvis is then manually "closed" to remove any surface holes with a lasso –add function in MIMICS.

The bone is wrapped and smoothed (3-5 mm) to close all superficial defects and remove all superficial imperfections. This is done to limit the number of elements in the meshing process without changing the stress distributions substantially.

The cup reamer assembly is then constructed in Pro- Engineer with a revolving extrusion. The reamer consists of a hemisphere attached to a cylinder (Figure 22). The reamer diameter is equivalent to the reamer diameter used in the pelvic reaming. Similarly, the cup diameter is the same diameter as the real cup placed in the hemipelvis. The reamer and cup are collinear so that once the reamer is placed the cup can be moved along the same axis to maintain the proper position (Figure 22). After creation in ProEngineer the cup reamer assembly is saved as an STL file for later import into 3matic.

A solid model of each "boxed" hemipelvis with the acetabular cup in place is created from CT scan. DICOM images are imported into MIMICS to create the solid model (Figure 23). This model will used to guide placement of the acetabular cup model so that it reflects the physical cup insertion. This will also allow determination of the nodes in the meshed model that

correspond to the LVDT sensors in the "boxed" hemipelvis. Both are critical for validation of the model.

The mask of each pelvis (with and without defect) in body frame of reference is imported into 3 matic. A second mask of the "boxed" hemipelvis pelvis with the cup in place is imported into 3 matic so that the virtual reaming and cup placement can mimic the actual cup placement. Once the proper position is ascertained the second mask is deleted. A cup reamer is then imported into 3 matic and inserted into the pelvis to the proscribed depth. A Boolean is performed to mimic reaming. The virtual reamer is 1 mm less in diameter than the virtual cup. A primitive plane is created for subtraction and the reamer is separated from the cup inserter assembly. The reamer is then deleted. The cup inserter assembly is left in place. The cup is one mm larger than the reamed acetabulum. The cup is now visibly protruded into the acetabulum.

The cup is now withdrawn along its axis so that the cup in barely touching the acetabulum. Eight different cross sections are viewed to ascertain that the cup is not protruded into the acetabulum at any point. The distance from the apex of the cup to the apex of the reamed acetabulum is measured. This is the distance that the cup will be pushed to fully seat the cup into the acetabulum.

At this time initial placement of the cup is complete. The cup and acetabulum must now be meshed in 3matic returned to MIMICs and saved as an ANSYS compatible file (Figure 24).

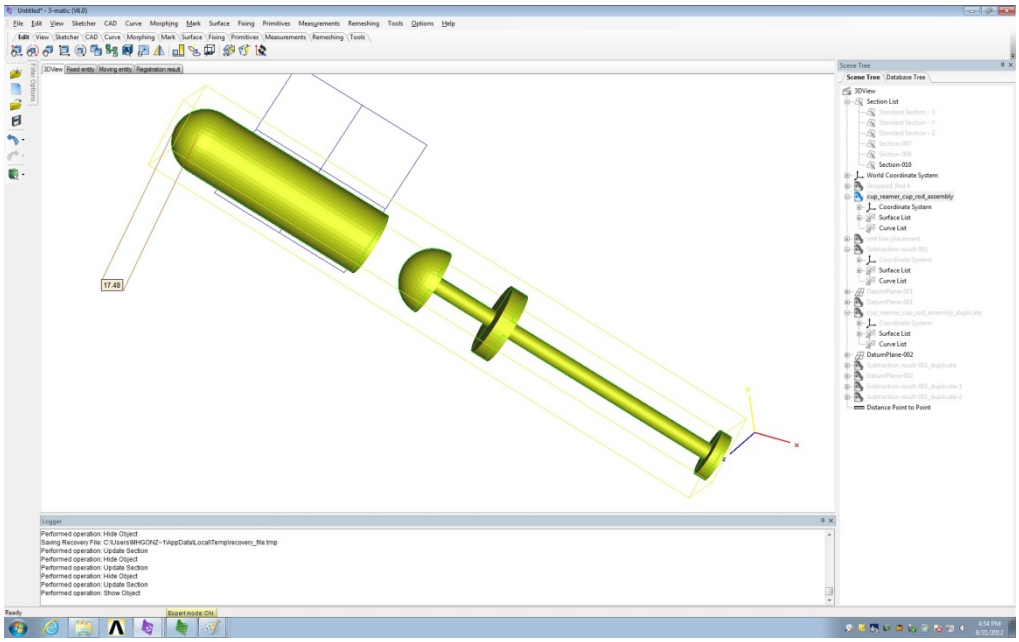

Figure 22 - Cup and Reamer created in Pro Engineer and Imported into 3Matic.

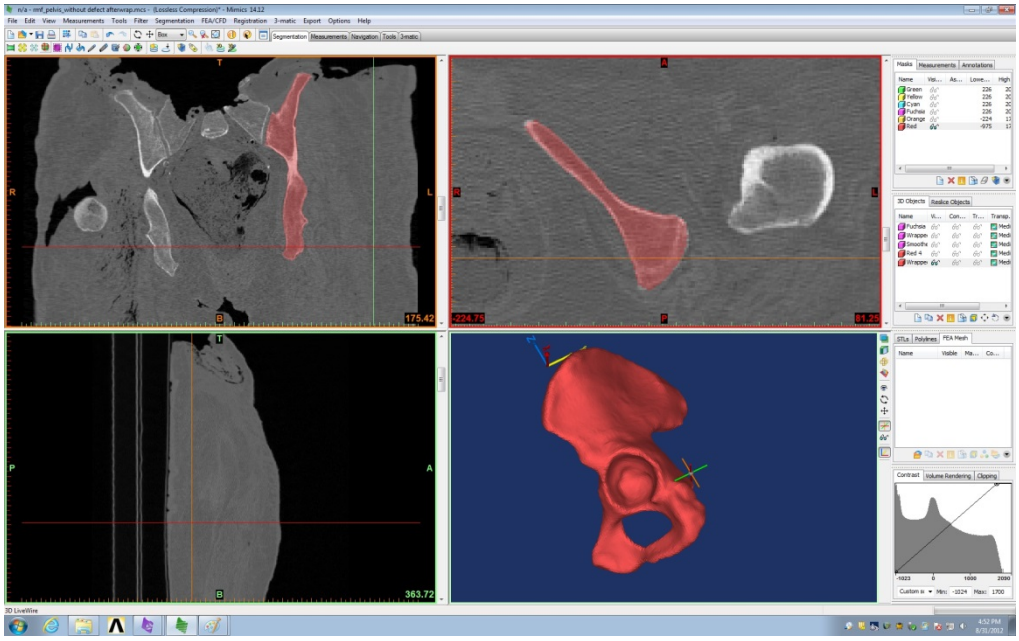

Figure 23 - Model of hemipelvis in MIMICS. Segmentation has been performed to isolate the hemipelvis from the contralateral hemipelvis.

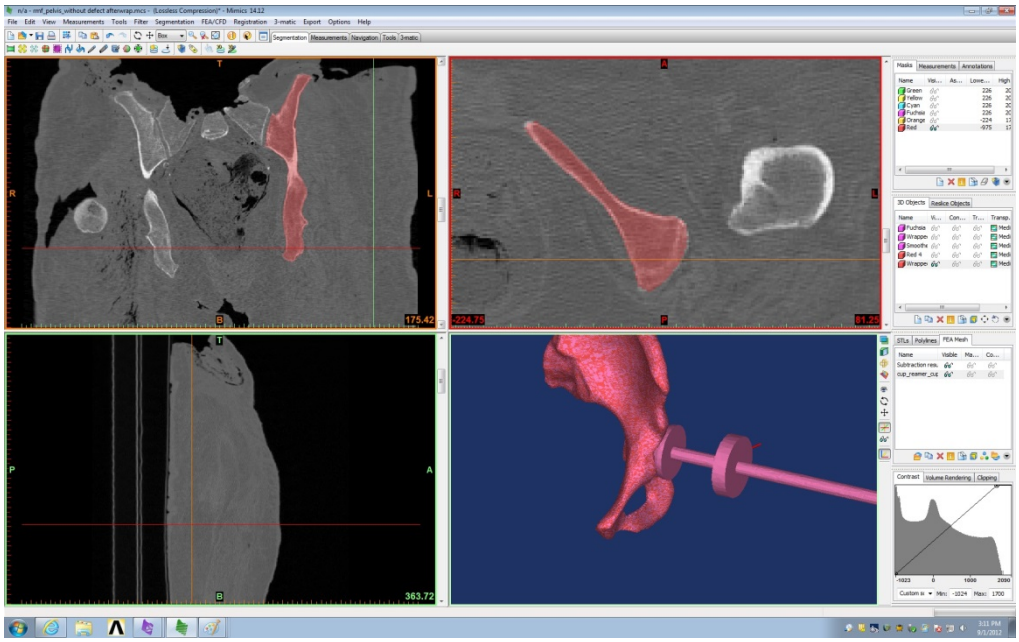

Figure 24 - Mimics model of acetabulum with cup in place. Note anatomic position of the cup and inserter which is used to apply prescribed loads.

CHAPTER 9 – FEA, Meshing, Boundary Conditions, and Loading

The pelvis and the cup with inserter 3D model is imported from MIMICS into ANSYS. The pelvis is fully constrained in the ischium and pubis modeling the experiment. The element type is Solid 72 which is a 4 node tetrahedron structural solid. This model is selected because it is useful for relatively irregular meshes such as a bone model. A coefficient of friction was set at 0.3 and the Young's Modulus for the cortical bone was set at 20,000 and for cancellous at 10,000. The cup is bonded to the acetabulum at a limited surface (see CHAPTER 7 – Development of the Model). The loading profile consisted of a combination of compression and torque produced by loading the cup off axis mimicking the experimental setup.

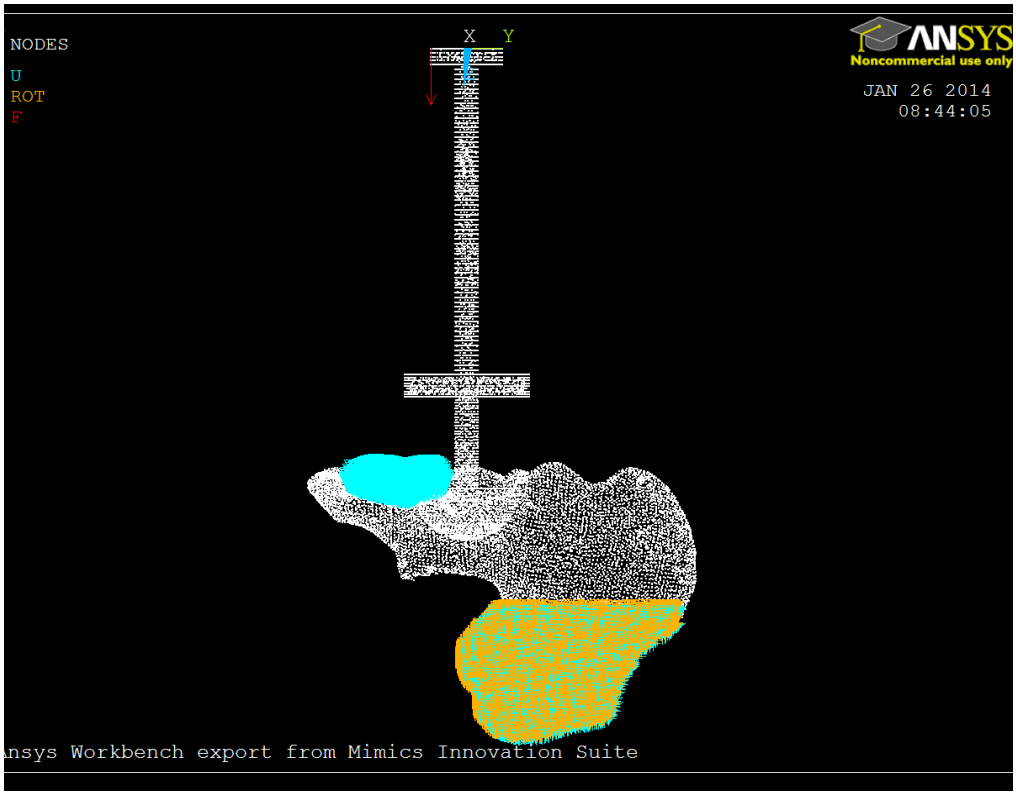

Figure 25 - Diagram noting the constrained nodes of the pelvis (Ischium and Illium) as well as the application (red line) of the compressive force.

In the first experiment the cup is constrained to the acetabulum at a varying number of nodes (bands). The cup is then loaded in 200 Newton increments from 0 to 3000 Newtons (Figure 25). The micromotion is measured by taking the micromotion readings at 3 nodes superior inferior and anterior and the tilt of the cup is calculated in the superior inferior and anterior posterior planes. The experimental results are compared to the results of the cadaver experiment to validate the experiment. The experiment is repeated for different degrees of constraint (4, 6, 8 bands). Two scenarios where the nodes are decreased either on the rim or equatorial side are analyzed. This is discussed in *CHAPTER 12 – Investigation of Cup Bone Fixation and Stability vs Defect Location*.

Table 3 - Percent of Nodes Constrained with Different Bands

Bands Constrained	Ratio of Constrained Nodes	Percent Constrained Nodes
8band	268/1161	23.10%
6band superior	189/1161	16.30%
6band inferior	216/1161	18.60%
4band superior	111/1161	9.60%
4band middle	137/1161	11.80%
4band inferior	157/1161	13.50%

In the second experiment the model is imported into Hypermesh and defects of the acetabular rim are created. The rim circumference is divided into eight equidistant defects (Figure 26). The defects are spaced 45 degrees apart and are roughly 1.5 cm in width and depth. The exact percentages of the total constrained nodes contained in each defect ranges from 17% to 23% and vary because some of defects fall in an inferior location where fewer nodes are

constrained. The models are reimported into ANSYS and the experiment repeated with the same loading profile.

Table 4 - Percentage of Constrained Nodes in Defect Model 1-8

Defect Number	Ratio (Nodes constrained)	Percent Constrained Nodes
1	208/1161	17.91559001
2	210/1161	18.0878553
3	219/1161	18.8630491
4	248/1161	21.36089578
5	268/1161	23.08354866
6	256/1161	22.04995693
7	185/1161	15.93453919
8	206/1161	17.74332472

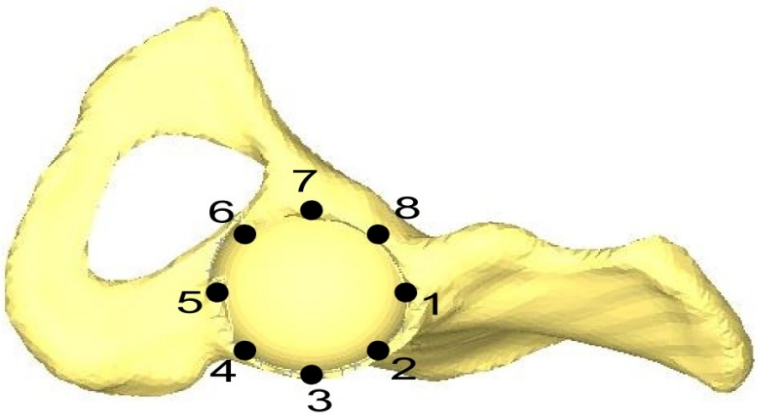

Figure 26 - Position of Defects 1-8. The defects are spaced 45 degrees apart. Defects 1 and 5 are along the primary axis which connects the anterior superior iliac spins and the ischium. Defects 3 and 4 are in the anterior column and defects 3 and 4 are in the posterior column. Defects 5 and 6 are inferior to the columns.

The third experiment evaluated the effect of the size of defect on the cup stability. The model was imported into hypermesh and different size defects were created in the second and the

seventh position of defect (Figure 27 - Figure 29). These positions were selected because in the second position there are nodes constrained to the cup on both sides of the defect while in the seventh position there are constrained nodes on only one side of the defect. The experiment is then repeated with the same loading profile.

Table 5 - Percent of Nodes in Defects

Defect Size	Nodes Defect Position 7	Percent Defect Position 7	Nodes Defect Position 2	Percent Defect Position 2
Large	1025/1161	11.71%	1033/1161	11.02%
Medium	1091/1161	6.03%	1091/1161	6.03%
Small	1137/1161	2.07%	1136/1161	2.15%

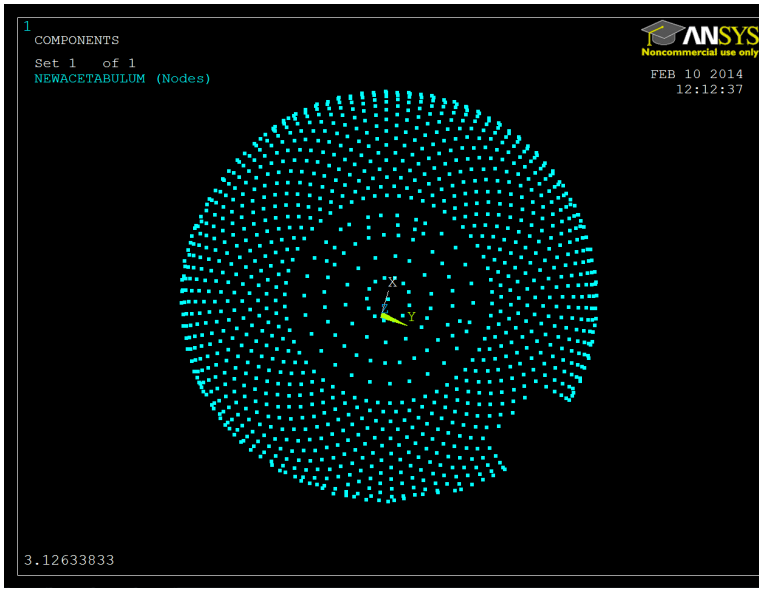

Figure 27 - Small Defect Position 2. 2.15 % of nodes from the surface are removed. Position 2 is a contained defect

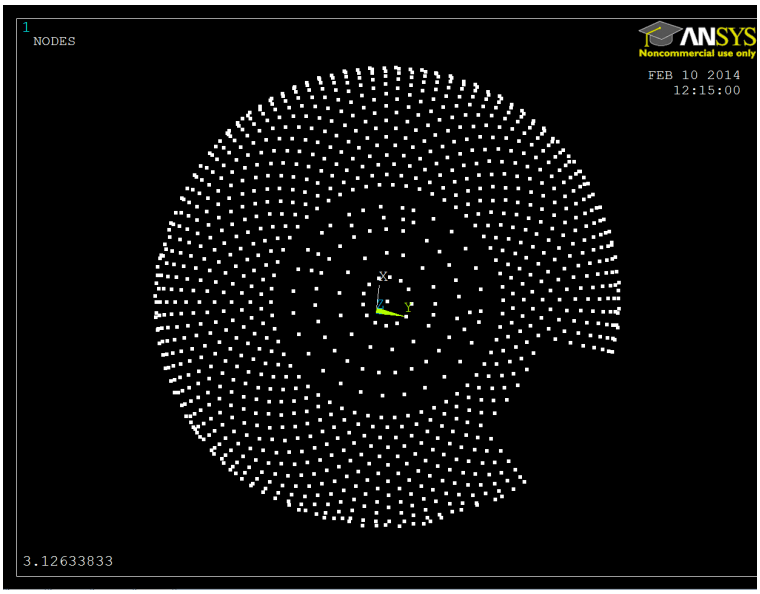

Figure 28 - Medium Defect Position 2. 6.03% of nodes from the surface are removed.

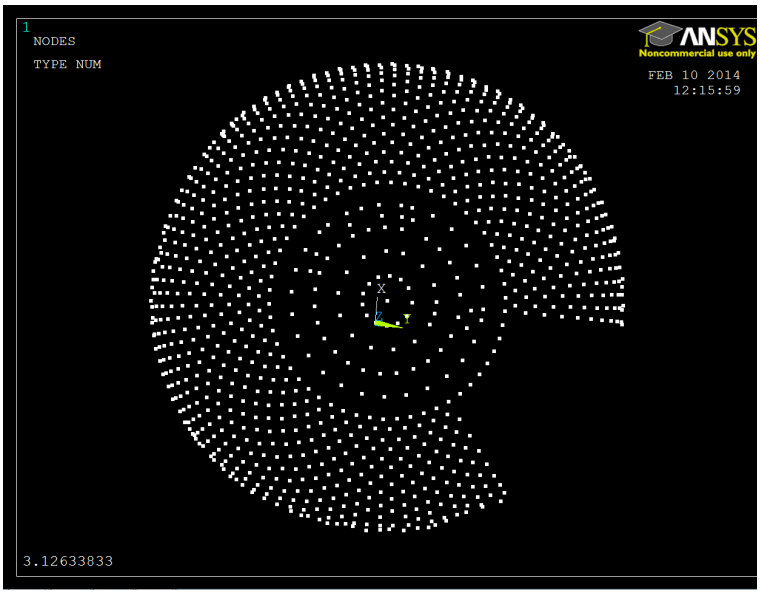

Figure 29 - Large Defect Position 2. 11.02% of nodes from the surface are removed.

The FE models used in the simulations are all based on a press-fit acetabular component and incorporate linear optimized material and bounded contact. The model was loaded with a road loader similar to the experimental setup used in the validation of the FEA model where loads of 1600 and 3000 N (3-4 X Body Weight) simulating one leg stance during fast walking and the second load was used as a testing load of failure.

CHAPTER 10 – Validation of the Model

The model has been previously validated in our laboratory and reported with 18 cadaver experiments [10] [76]. For the particular model which is patient specific, the cadaver test was repeated.

A male human cadaver was obtained and a CT scan of the pelvis was taken. The bilateral hips were exposed and a 1.5 cm defect was created in the right acetabulum, analgous to the first defect of the virtual pelvis (see CHAPTER 14 – Discussion). The acetabula were reamed and a cementless cup was placed bilaterally. A CT scan was then performed of the pelvis to ascertain the position of the acetabular cups.

The hemipelvis with the acetabular components was harvested and placed in the testing jig as described in *CHAPTER 8 – Computer Modeling of the Acetabulum Based on CT Data Using CAD/MIMICS*. Micromotion was tested by three LVDT sensors placed superiorly inferiorly and anteriorly. Each acetabular cup was loaded with a loading profile as described in Chapter 8. The relative micromotion was calculated both in the Superior inferior and anterior posterior planes.

A virtual model was created of the same pelvis both with and without the defect. The component was placed in an identical position as defined by the CT scan. An identical loading profile was then applied to both the acetabulum without a defect and that with a superior (position1) defect. The relative micromotion was calculated again in the superior inferior and anterior posterior planes. The values were plotted of the experimental and the virtual model values.

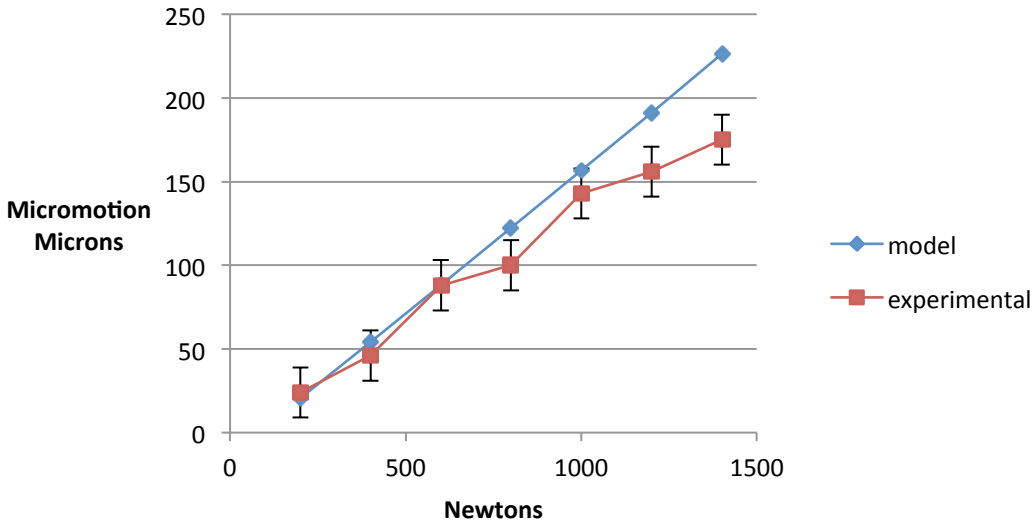

Figure 30 - Acetabulum without defect superior inferior micromotion. There is very good correlation at smaller physiologic loads .

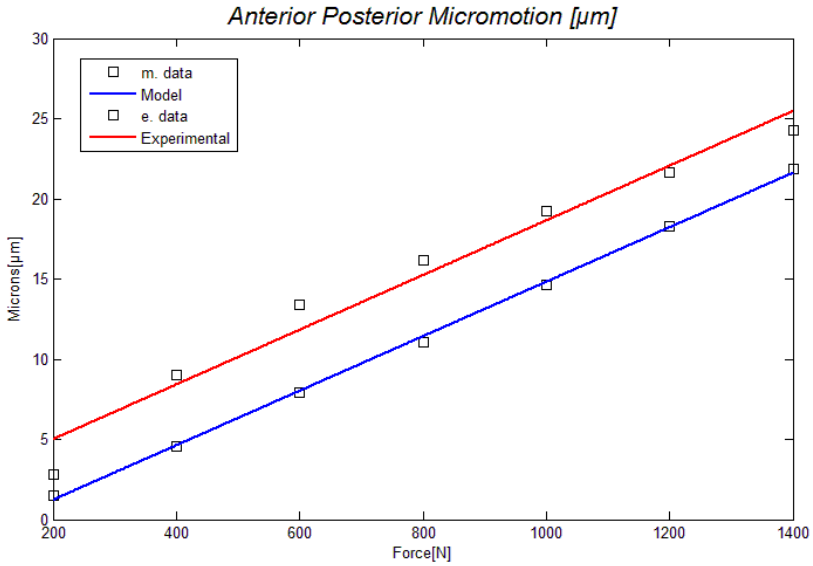

Figure 31 - Acetabulum without defect anterior posterior micromotion. The anterior posterior motion is at or below 5 microns in both model and experiment.

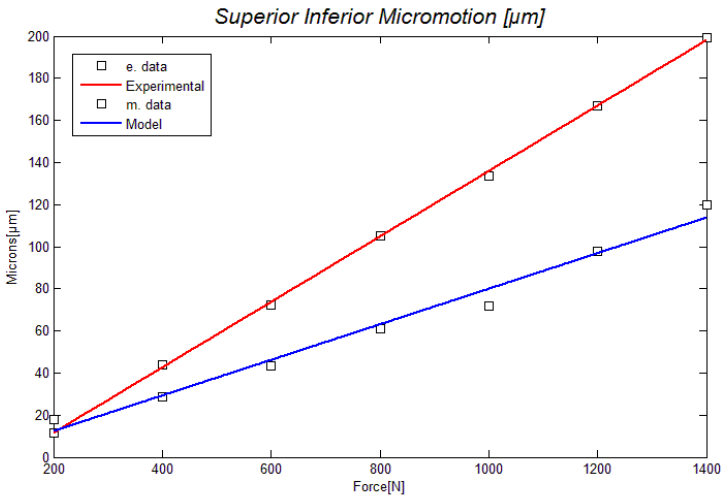

Figure 32 - Acetabulum with defect superior inferior micromotion. There is some divergence of the graph at loads that are supra physiologic.

A good correlation is noted between the micromotion values for the acetabula without a defect. The LVDT sensor has an error of +/- 15 microns. All the superior inferior values are within 25 microns up to 800 Newtons and within 50 microns with 1400 Newtons of force (Figure 30). Five of the 7 data points fall within the tolerance of the sensor. The anterior –posterior micromotion shows that the values are within 15 microns up to 1400 Newtons (Figure 31).

In the case of the acetabulum with a defect the superior inferior values are within 50 microns up to 800 Newtons (Figure 32). It is extremely difficult to create an exact defect in the model that mirrors the experiment. This is primarily due to difficulty in placing the cup in the exact position as in the side without the defect and the difficulty of localizing the defect because of scatter in the CT scan.

CHAPTER 11 – Analysis of Various Contacts Conditions and Bonding between the Cup and Acetabulum Wall

In this thesis research the finite element method (FEM) was used as a tool to analyze the effects of fully bonded implant-bone interface assuming total ingrowth of the cup. The bounding is described as a varying band with different depth and account for the numbers of nodes are assumed bounded within the contact surface. The FE model of the press-fit acetabular component incorporates non-linear material and allows the bone to deform in accordance with the constraints imposed. The model was loaded with a compressive load coupled with a torque similar to the ones induced by the abductor hip muscles. Although the hip is a concentric joint with primarily compressive force torque is applied to the cup when the femoral neck impinges on the cup at the extremes of motion. Torque is also applied when in the relaxed state and the ball and cup become dissociated. Upon reduction the femoral head can impart a moment onto the cup before it becomes centered in the acetabulum.

The initial condition was binding of the eight equatorial bands of nodes which amounted to 23.1% of the nodes on the inner surface of the acetabulum (Figure 33).

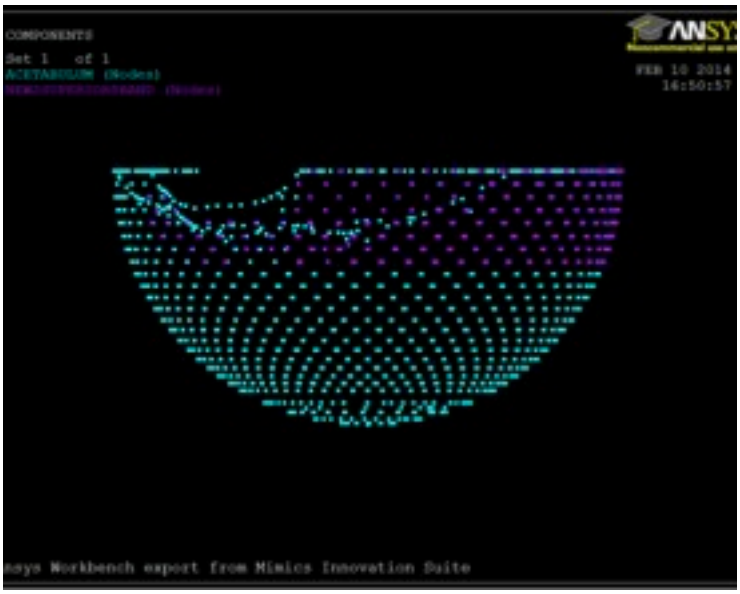

Figure 33 - 8 Band (23.1% of nodes constrained).

The bands were then decreased on the rim to 6 bands (16.3% of nodes constrained) and 4 band (9.6% of nodes constrained). The bands were decreased on the equatorial (rim) side (Figure 34 and Figure 35).

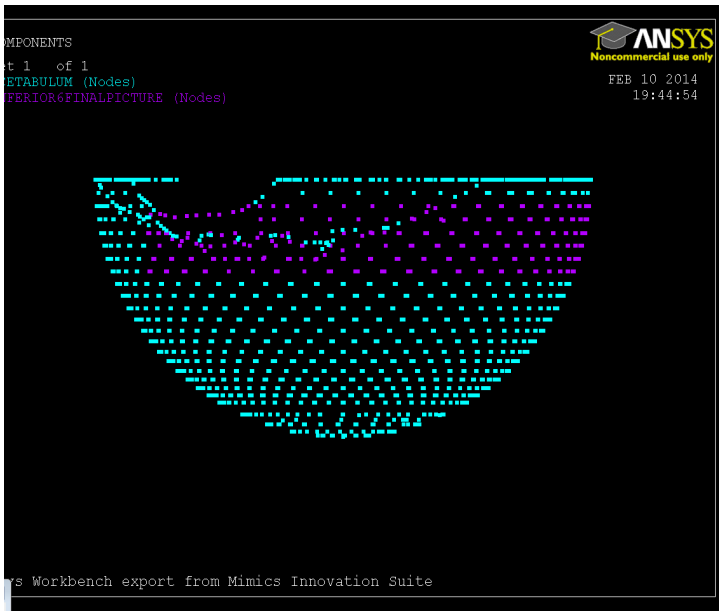

Figure 34 - 6 Band Inferior (18.6% of nodes constrained). Two bands of nodes at the equator are no longer constrained.

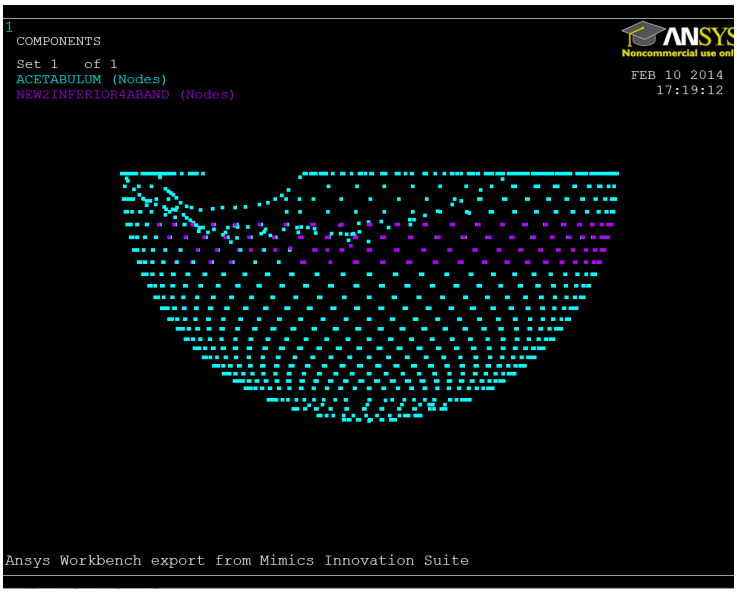

Figure 35 - 4 band Inferior (13.5% of nodes constrained). Four bands of nodes at the equator are no longer constrained.

Micromotion increased substantially as the number of bands were decreased (Figure 36).

At 1600 hundred N the peak stresses showed slight differences between the 4 and 8 band

construct. At 3000 N there were significant differences with the 4 band construct showing very high peak stresses 160 vs 90MPA (Figure 37 - Figure 40).

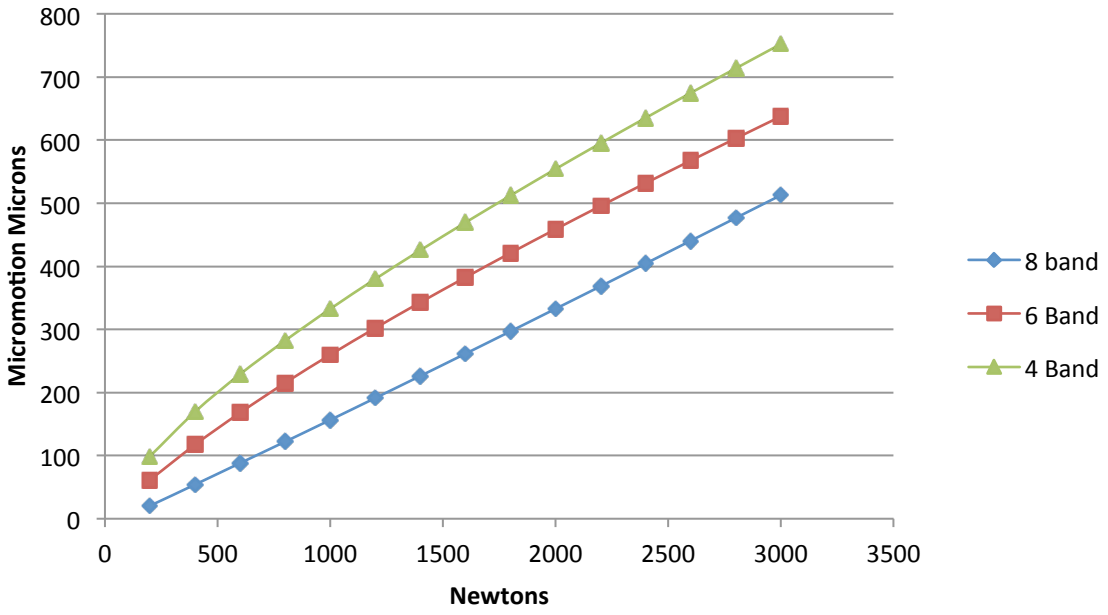

Figure 36 - Micromotion Comparing 4, 6, 8 Bands inferior Constrained. Loss of equatorial fixation of the cup increases micromotion.

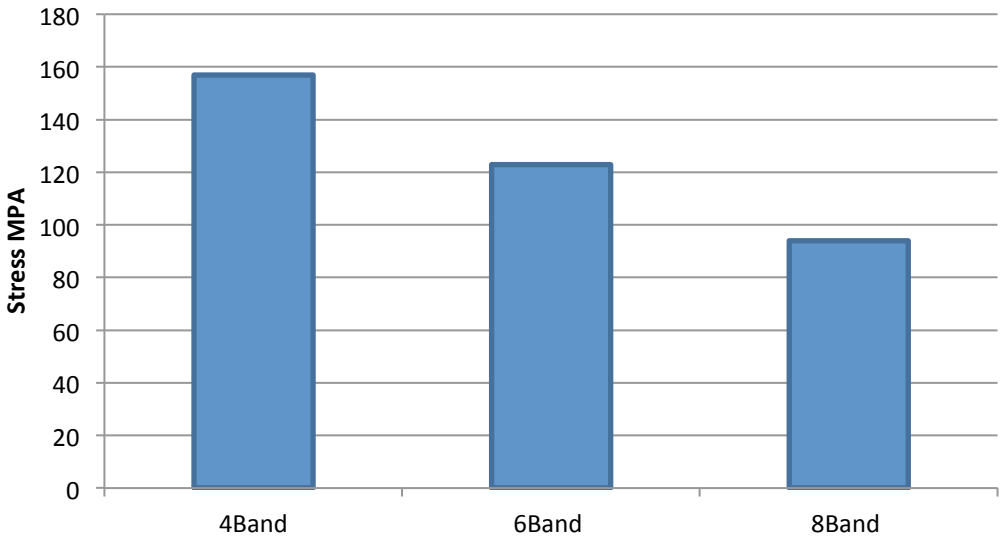

Figure 37 - Peak Stresses MPA 3000 Newtons. A decrease in equatorial fixation is associated with an increase in peak stress.

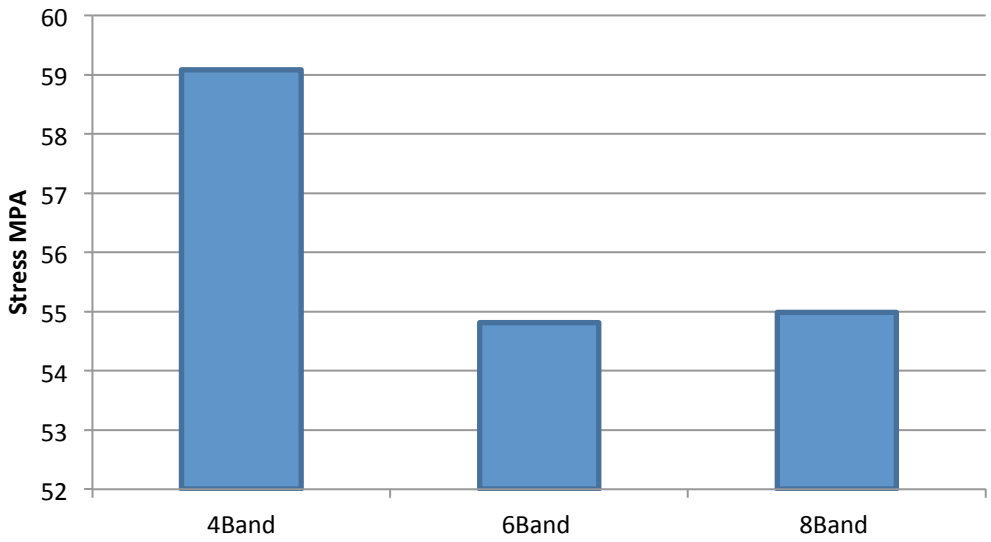

Figure 38 - 200 Highest Nodes Average Stresses 3000 Newtons. A decrease in equatorial fixation is associated with an increase in peak stress.

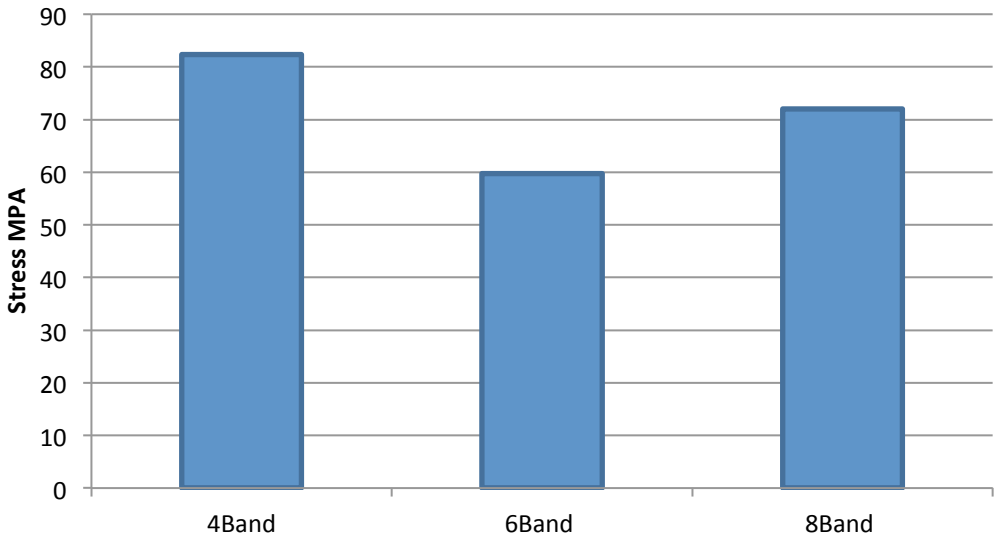

Figure 39 - Peak Stresses MPA 1600 Newtons. A decrease of 4 bands of fixation in the equator is associated with increased peak stress at 1600 Newtons.

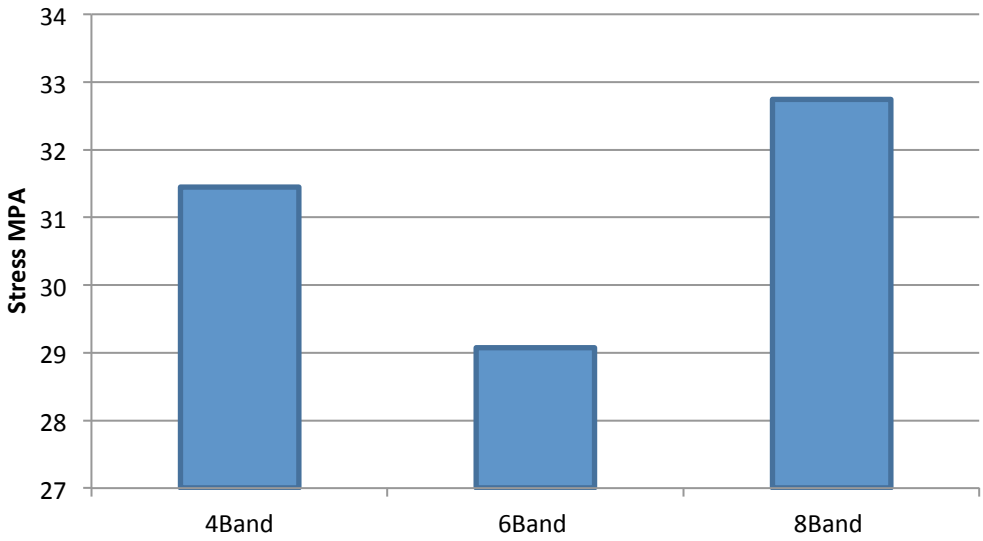

Figure 40 - 200 Highest Nodes Average Stresses 1600 Newtons.

In the second scenario the bands were removed from the dome side (Figure 41 and Figure 42). There proved to be little micromotion difference between the 6 and 8 band construct, but there was a substantial increase in micromotion with the 4 band construct (Figure 43). At both 1600 and 3000 N the shear stresses showed a marked increase between 4 and 6 bands (Figure 44 - Figure 47).

Decreasing the number of bands on the equatorial side of the contact surface is analgous to the decreased radius cups which are used with a monoblock metal on metal design. These cups showed a high incidence of early failure because of a lack of fixation and failure of bone ingrowth. In our model the 4 band model failed showed increased instability which may explain why in practice these cups failed.

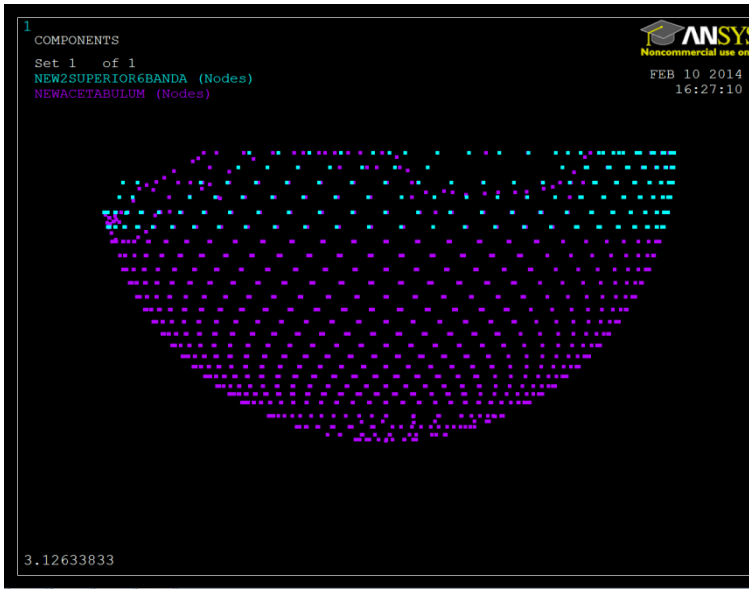

Figure 41 – 6 Band Superior (16.3% of nodes constrained). 2 Bands are removed from the dome side of the cup.

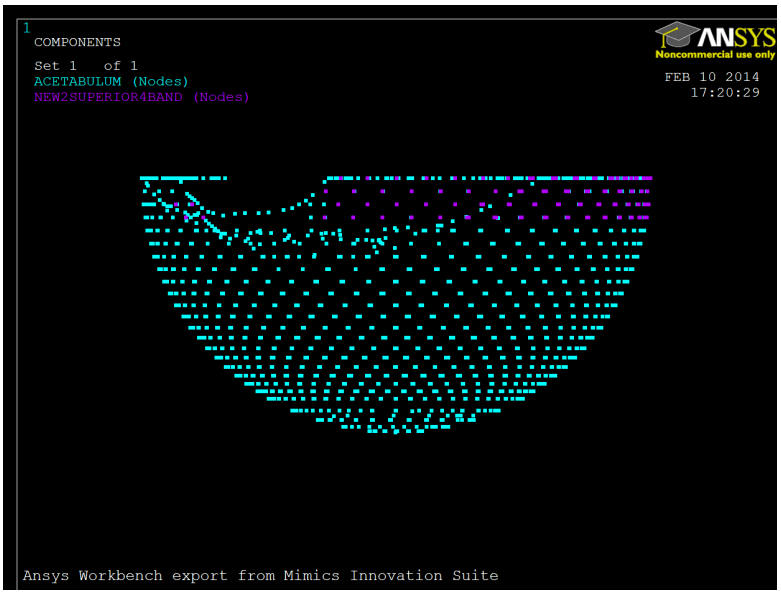

Figure 42 - 4 Band Superior (9.6% of nodes constrained). 4 Bands are removed from the dome side of the cup.

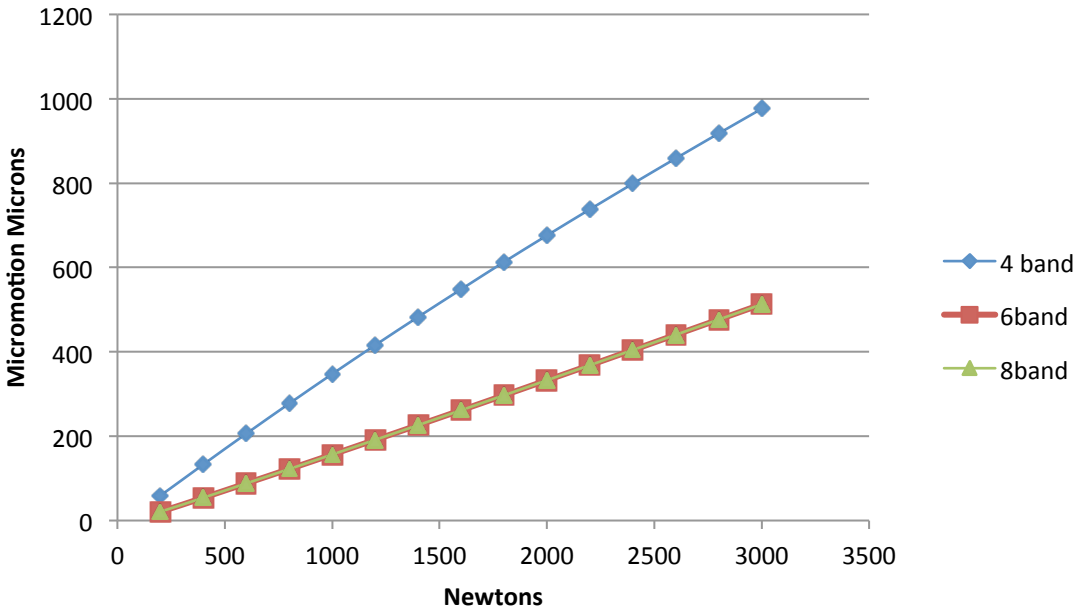

Figure 43 - Micromotion Comparing 4, 6, 8 Bands Superior Constrained. Removal of 2 bands has little effect but removal of 4 bands causes a marked increase in micromotion.

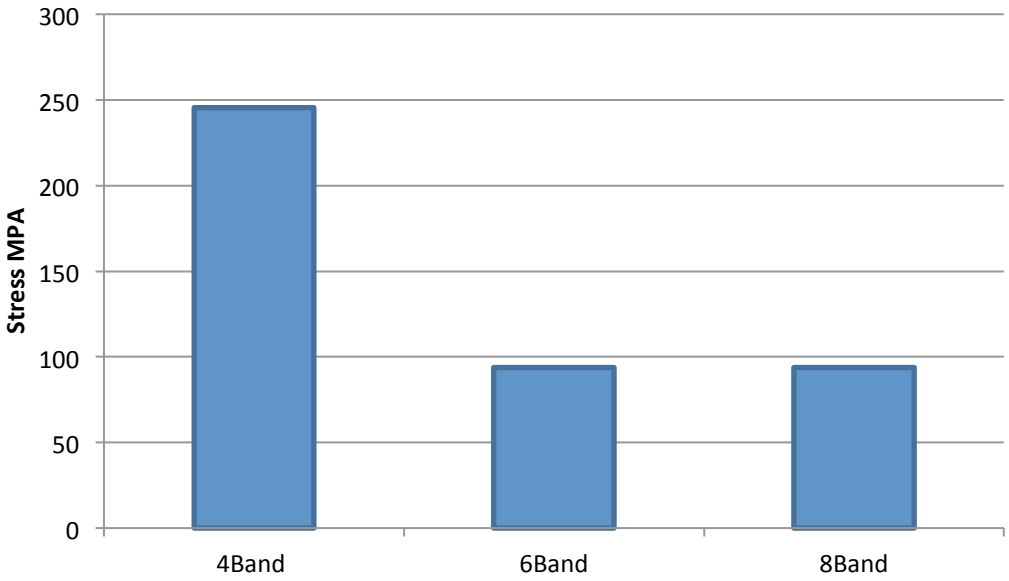

Figure 44 - Peak Stress MPA 3000 Newtons. Removal of 2 bands shows little change in peak stresses but removal of 4 bands causes a significant increase in peak stresses.

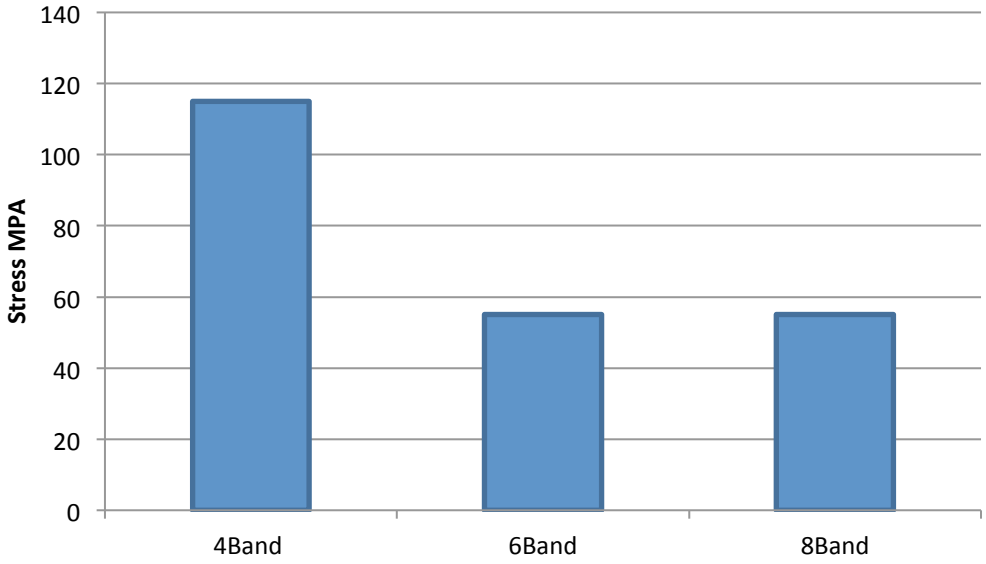

Figure 45 - 200 Highest Nodes Average Stresses 3000 Newtons. Removal of 2 bands shows little change in peak stresses but removal of 4 bands causes a significant increase in peak stresses.

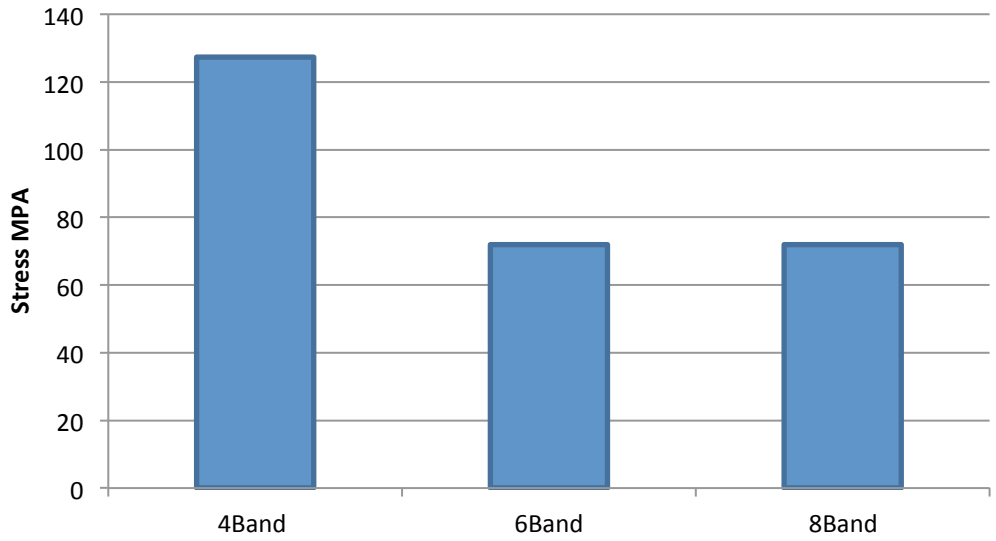

Figure 46 - Peak Stresses MPA 1600 Newtons. Removal of 2 bands shows little change in peak stresses but removal of 4 bands causes a significant increase in peak stresses.

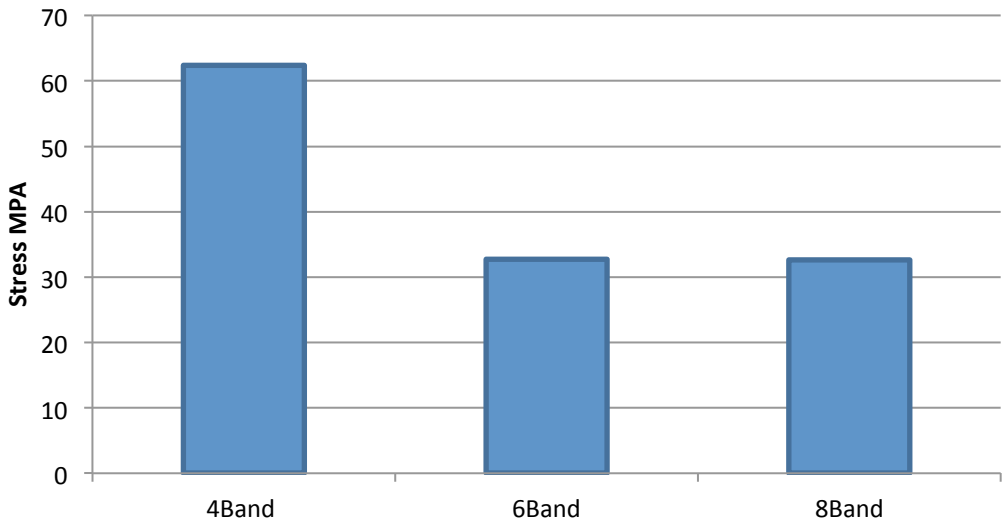

Figure 47 - 200 Highest Nodes Average Stresses 3000 Newtons. Removal of 2 bands shows little change in peak stresses but removal of 4 bands causes a significant increase in peak stresses.

CHAPTER 12 – Investigation of Cup Bone Fixation and Stability vs Defect Location

The defects have been placed in circumferentially in 45 degree intervals around the acetabular rim. The defects are wedged shaped and are roughly 15% of the entire circumference (Figure 48). The constrained nodes are placed in an equatorial arc in an inverted u covering about a 270 degree arc (Figure 49).

The defects can fall outside the arc of constrained nodes as noted in defect 5 (Figure 50), can fall at the edge of the arc and are uncontained as in defects 4, 6, 7 (Figure 51) or can be completely contained by the arc of constrained nodes defects 1, 2, 3, 8 (Figure 52).

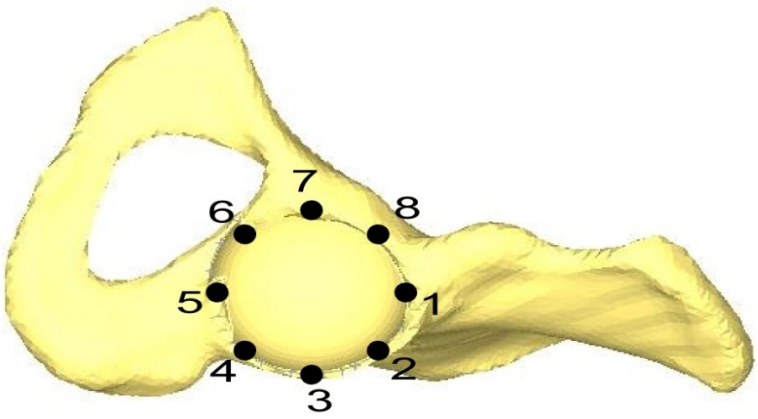

Figure 48 - Position of the Acetabular Defects. Position of Defects 1-8. The defects are spaced 45 degrees apart. Defects 1 and 5 are along the primary axis which connects the anterior superior iliac spins and the ischium. Defects 3 and 4 are in the anterior column and defects 3 and 4 are in the posterior column. Defects 5 and 6 are inferior to the columns.

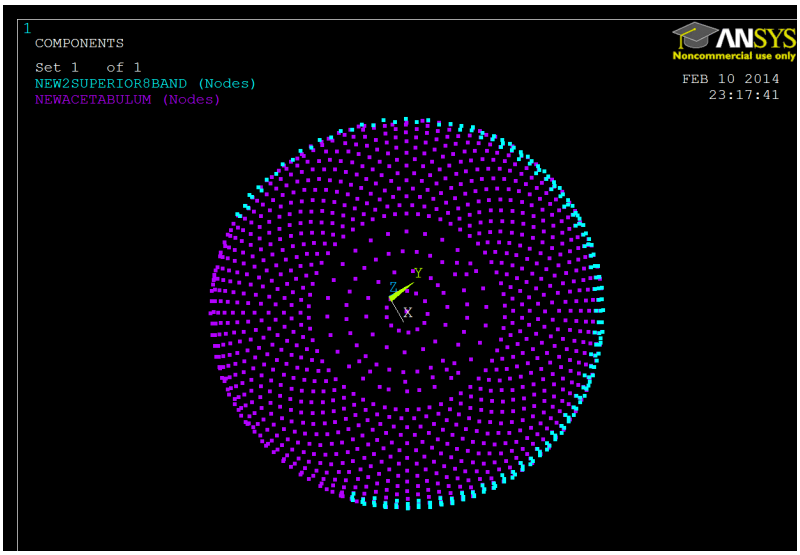

Figure 49 - Constrained Arc of Nodes of Acetabulum Without Defect. The portion of the cup at the acetabular notch is left unconstrained.

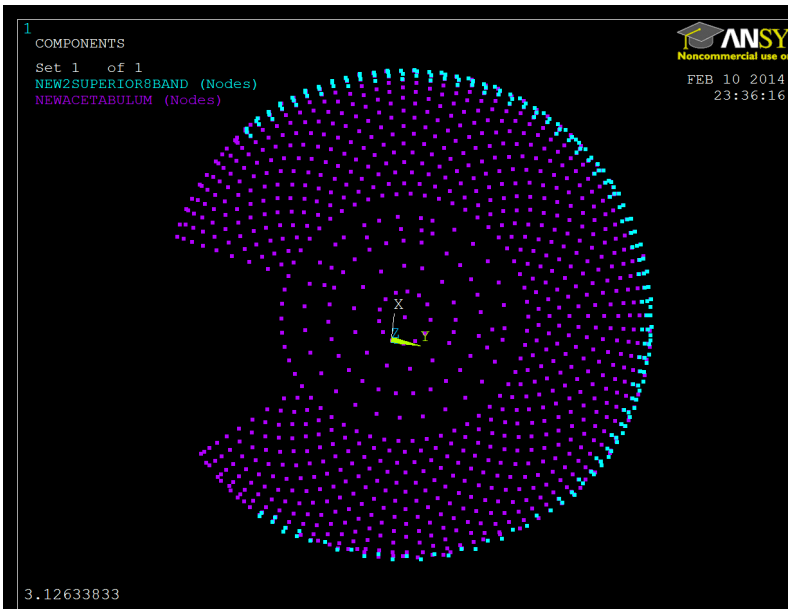

Figure 50 - Defect 5: The bone defect falls outside (inferior) to the arc of constrained nodes. The entire zone of fixation is maintained.

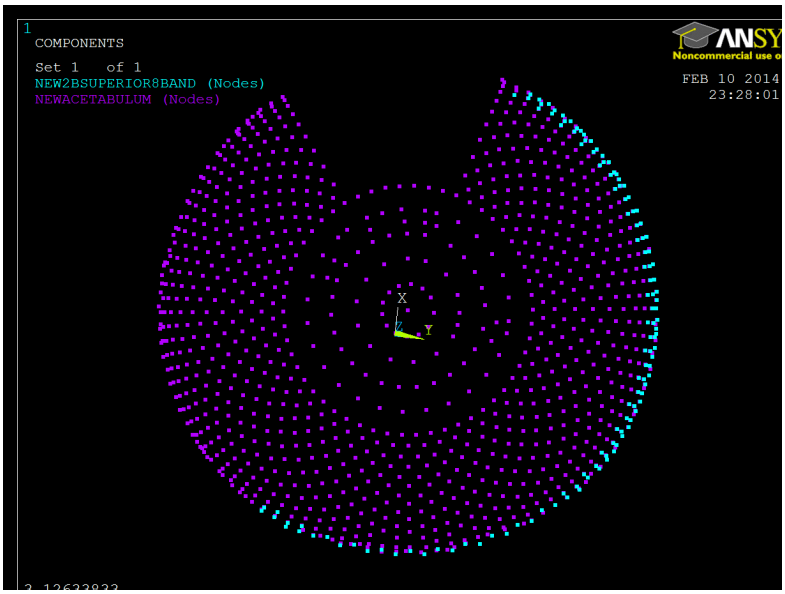

Figure 51 - Defect 7: The defect falls at the edge of the arc of constrained nodes and is uncontained. The defect is not bridged.

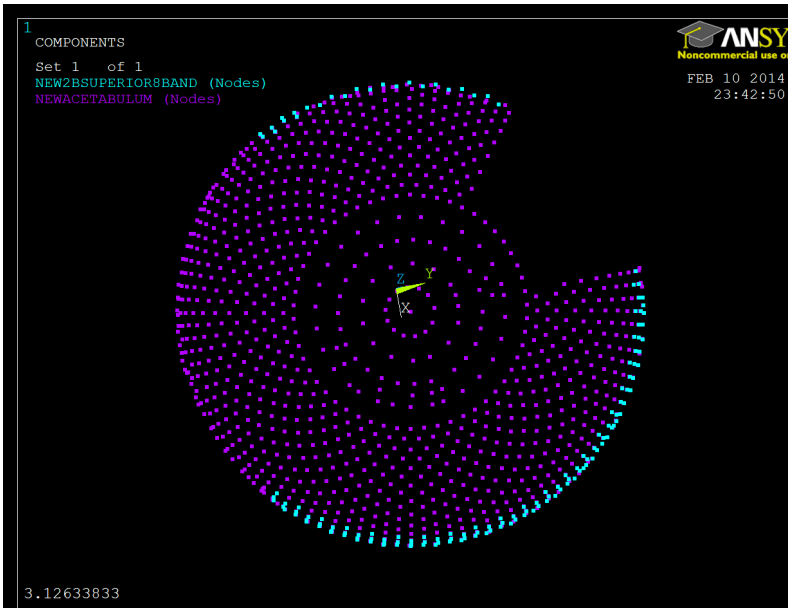

Figure 52 - Defect 2: The defect is contained (bridged) by the arc of constrained nodes.

The order of stiffness of the construct from most rigid to the one with the most micromotion was 1, 5, 2, 6, 8, 4, 3, 7 (Figure 53). Defects 1 and 2 are superior between the two columns and are bridged by the constrained nodes (Figure 54). Defects 5 and 6 are inferior and fall outside either of the columns (Figure 55). Defects 3 and 4 are in the posterior column (Figure 56). Defects 7 and 8 are in the anterior column (Figure 57). The defects exhibiting the most micromotion (7, 3, 4 respectively) fall within a column and are not bridged by the constrained nodes.

The peak stresses are generally highest in the defects 3,4,7,8 which are all in either the anterior or posterior column (Figure 58 - Figure 61). Defects outside the columns show overall lower peak stresses.

The areas of highest stress concentration are centered around the defect as evidenced by Figure 62 and Figure 63. Defect 1 lies between the two columns and is bridged by the constrained nodes of the cup minimizing the development of local stress (Figure 63). Defect 7 lies in the anterior column and is not bridged by the constrained nodes of the cup. This shows much higher stress centered about the defect (Figure 62).

A defect as a potential stress riser must be a consideration clinically. The propagation of a crack through a defect if not noticed can lead to a failure of fixation and early implant failure.

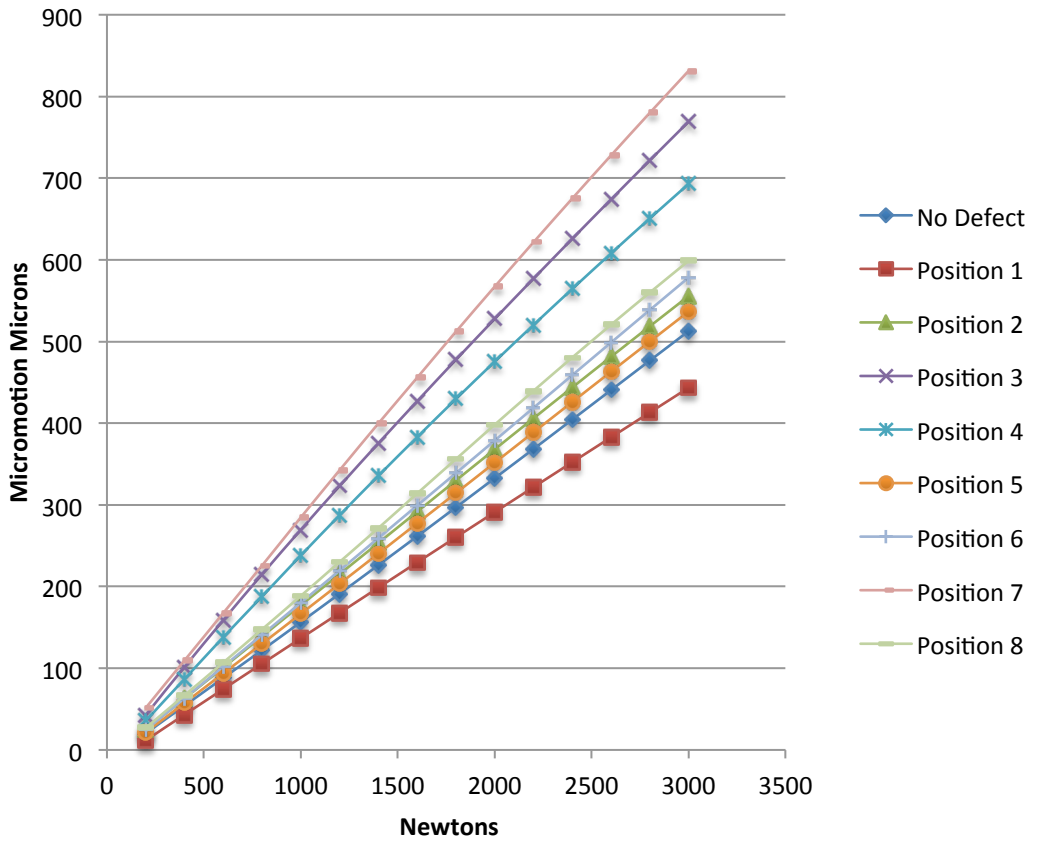

Figure 53 - The degree of micromotion of the acetabulum without defect and the eight defects. The order of stiffness from greatest to least is 1, 5, 2, 6, 8, 4, 3, 7. Defects 7 and 8 are in the anterior column and defects 3and 4 are in the posterior column. Defects 7, 3 and 4 are not bridged.

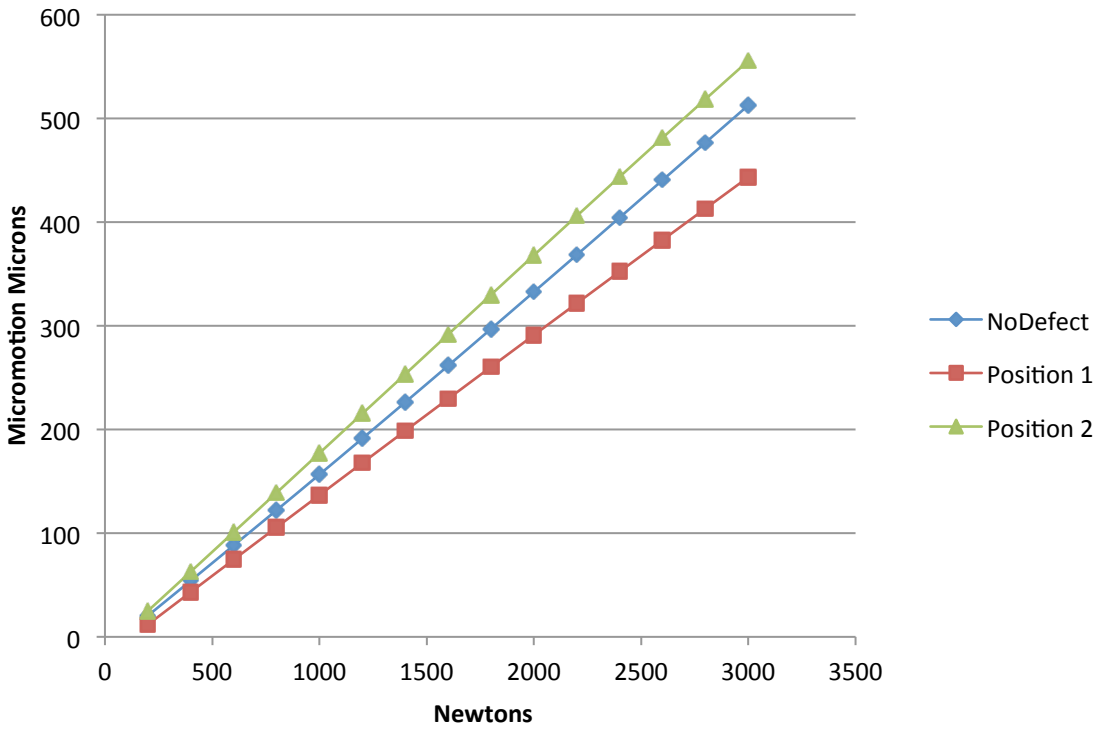

Figure 54 – Results of defects 1 and 2 which are both contained defects. Both defects fall outside the anterior or posterior column and are not structural.

Defects 1 and 2 are both contained defects and in both cases the anterior and posterior columns are largely intact. In fact the first defect shows greater stiffness than the intact bone.

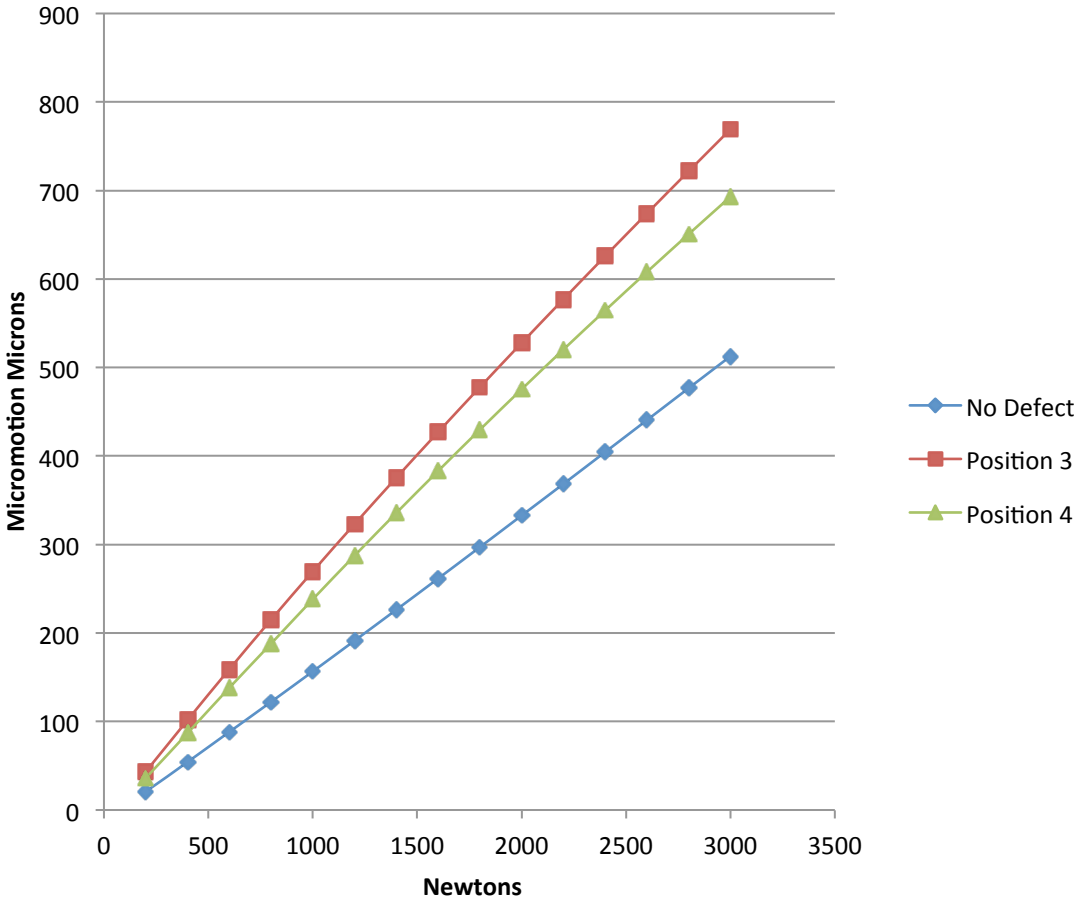

Figure 55 - Results of defects 3 and 4 which create a structural lesion in the posterior column. Both defects are not bridged by constraining nodes.

Defects 3 and 4 create a structural lesion in the posterior column. Both show substantially more micromotion than the 1st and second defects. Defect 4 is unconstrained but lies inferiorly almost within the ischium of the weight bearing column which may foster mechanical support making it slightly more rigid than the third defect.

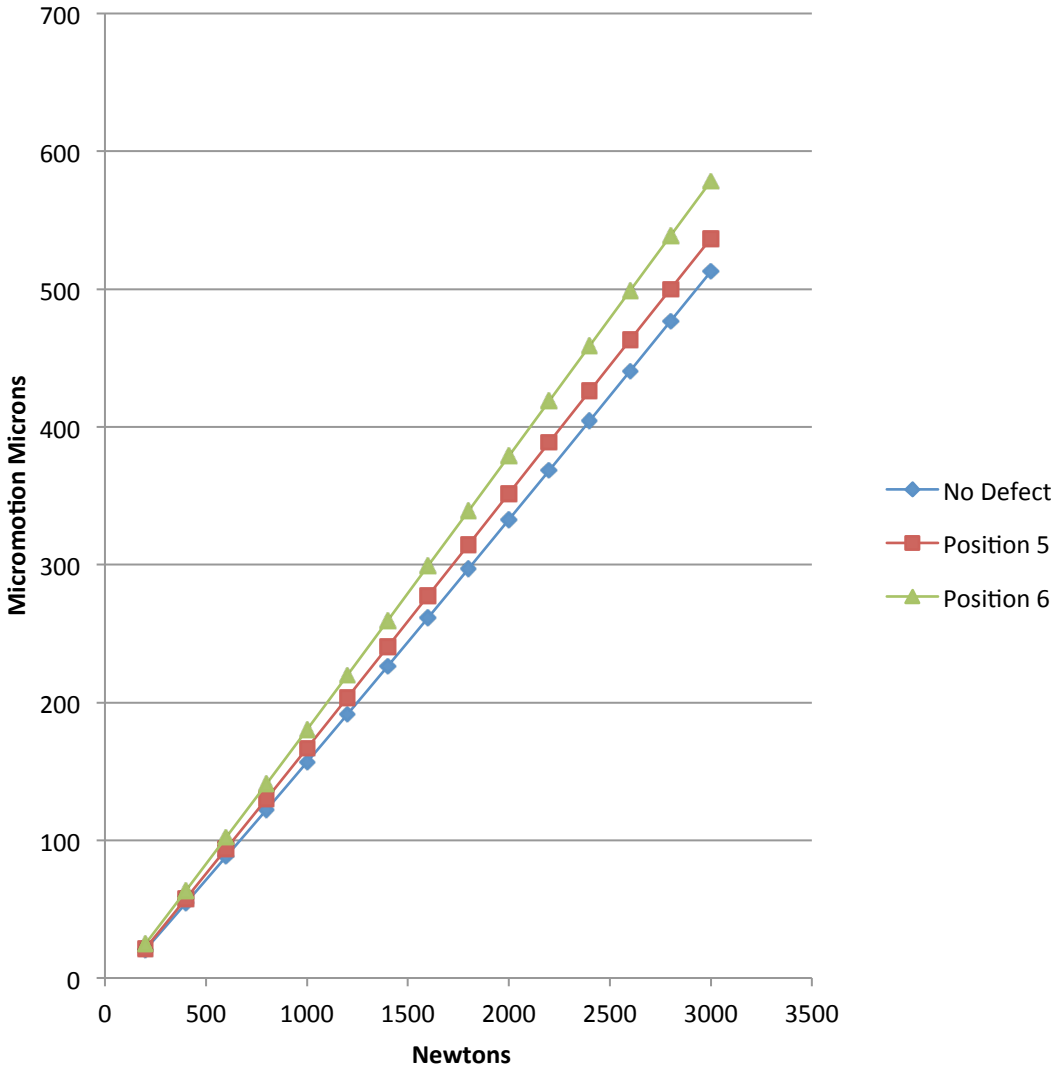

Figure 56 - Results of defects 5 and 6. Both defects are inferior to the columns and are non structural.

Defects 5 and 6 show virtually no micromotion increase as compared to the acetabulum without a defect. Both defects lie inferior to the columns of the acetabulum in an area that is unconstrained.

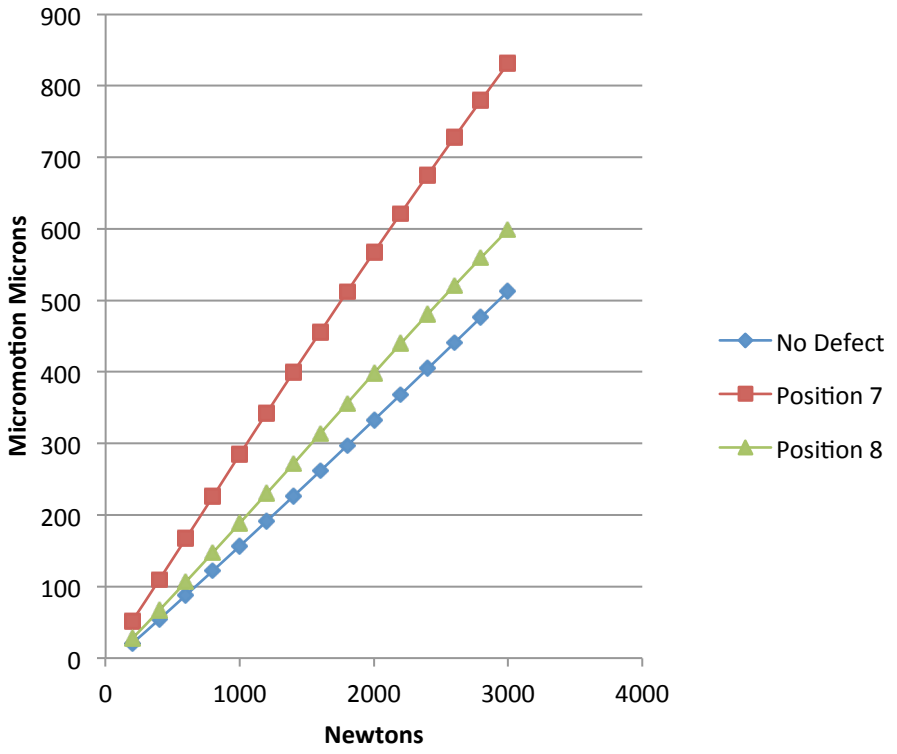

Figure 57 - Results of defect 7 and 8. Defects 7 and 8 are in the anterior column and are structural. Defect 8 is bridged by constraining nodes. Defect 7 shows the greatest micromotion of all defects and is both structural and unbridged by constraining nodes.

Defect 7 has the most micromotion of all the defects. The seventh defect creates a structural defect in the anterior column and is not bridged by the arc of constrained nodes. Defect 8 also creates a structural defect in the anterior column but is bridged by the arc of constrained nodes.

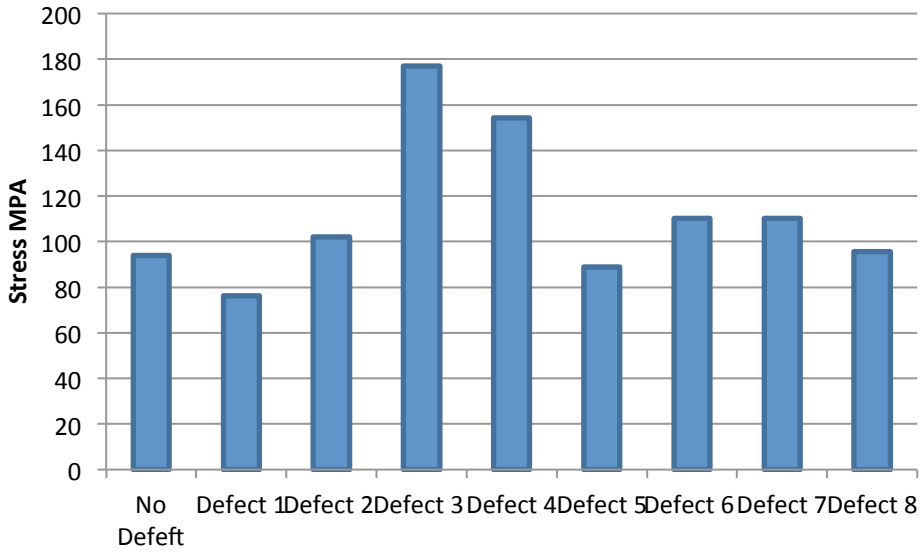

Figure 58 - 3000 Newton Peak Stress MPA for defects 1-8.

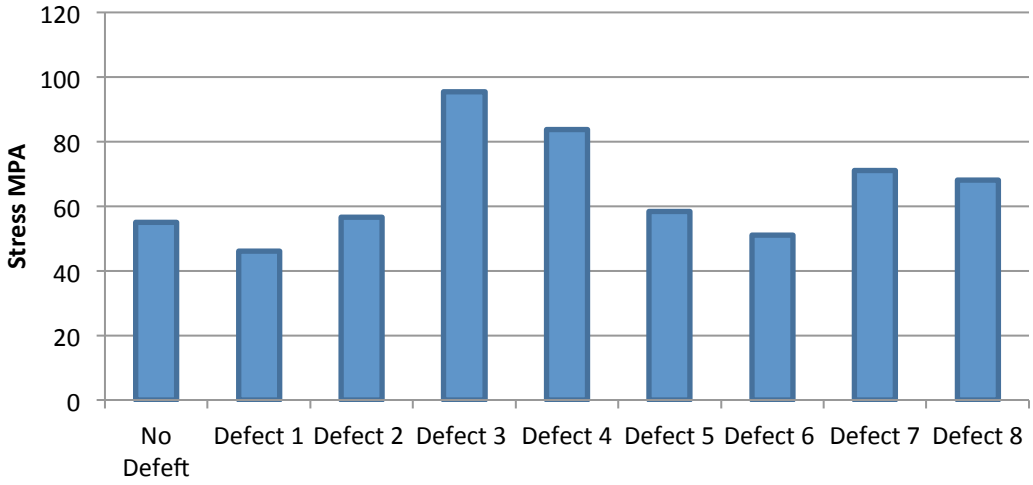

Figure 59 - 3000 Newton 200 Peak Node Average Stress MPA.

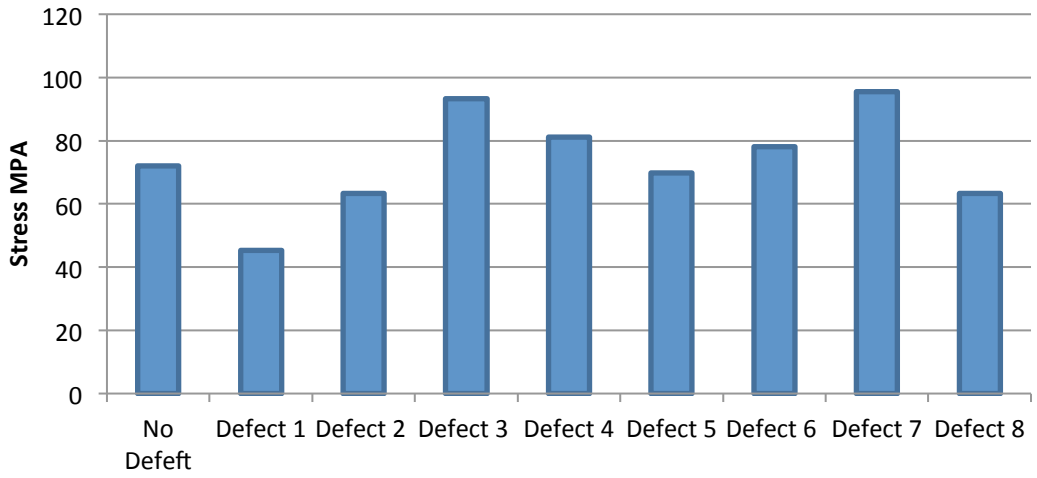

Figure 60 - 1600 Newtons Peak Stress MPA.

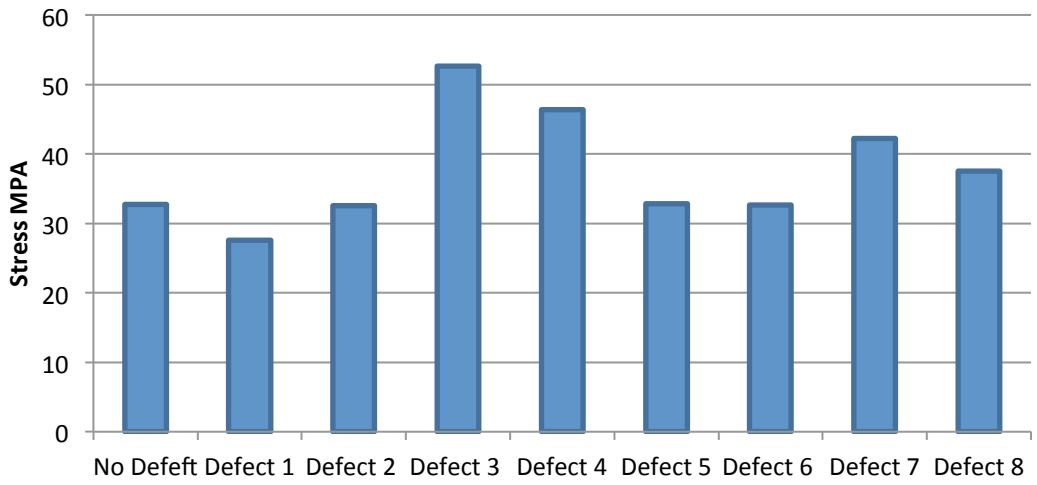

Figure 61 - 1600 Newton 200 Peak Node Average Stress MPA.

The highest peak stresses tend to be associated with those defects associated with the anterior or posterior column. The bar graphs show the peak stress and the average of the highest

200 nodes at both 1600 and 3000 Newtons. Defects that are superior or inferior to the columns tended to have smaller peak stresses.

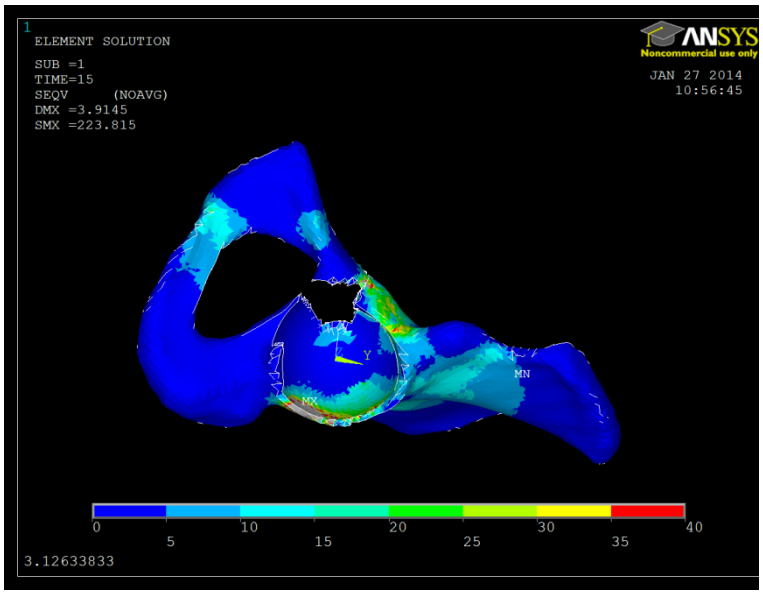

Figure 62 - Von Mises stress defect 7 - 3000N. Note highest peak stresses in the area of the acetabular defect and in the acetabular columns.

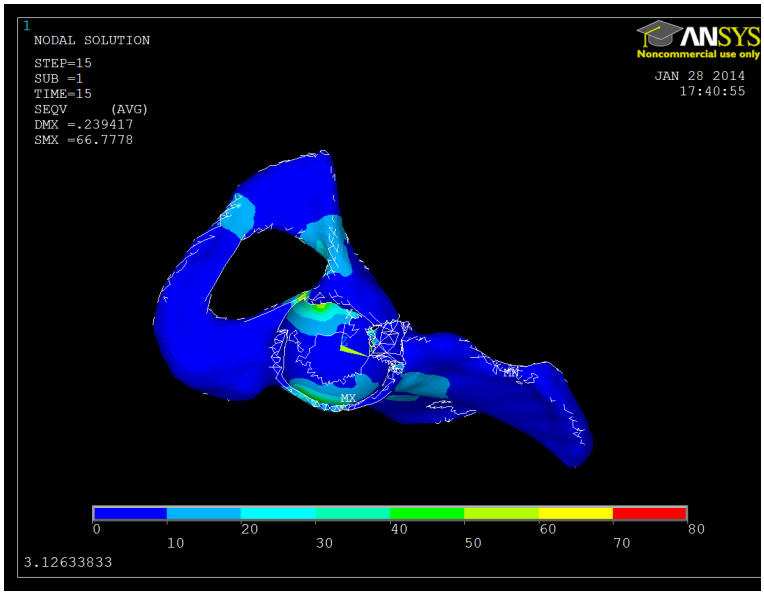

Figure 63 - Von Mises Stress defect 1 - 3000N. Note highest peak stresses in the area of the acetabular defect and in the acetabular columns.

Micromotion measurements as function of load for intact and 8 different defect positions are shown in Figure 53. The results show that the load varies linearly as function of micromotion displacements measured in all 3 axis. The intact acetabulum without defect (original acetabulum) shows a close behavior to a acetabulum with defects 1, 2, 6, 5, and 8 and cause a linear deformation transferred to the periphery of the side walls, especially to the acetabular cortical rim whereas the subchondral bone is exposed to lower, predominantly meridional (tension) stresses. Defect 3, 4 and 7 show much higher micromotion in excess of 25% greater than the intact bone or other defects. Higher loads are true indicators of defect failures as they correspond to greater stresses above the normal yielding stress of the bone, hence resulting in loosening and complete failure of the cup.

Defects of the anterior or posterior columns show more micromotion than defects that are superior or inferior. Defects 1, 2, 5, and 6 are relatively nonstructural and show minimal micromotion. Defects that are bridged tend to show less micromotion than defects that are unconstrained. Unconstrained defects also show local peak stresses much higher than constrained defects. This is critical because unconstrained defects are a stress riser that can potentially lead to acetabular fracture.

CHAPTER 13 – Investigation of Cup Bone Fixation and Stability versus Defect Size

The cup stability was evaluated when varying size of bone defects were present. The defect sizes were small (3.9%) medium (7.5%) and large (13%). The percentages are the percent of nodes removed divided by the total number of contact nodes on the surface of the acetabulum. The position of the bone defect was compared in the second and seventh position (Figure 64). The second position is bridged by bound nodes on both sides of the defect. The seventh position is not bridged by bound nodes and is inferior.

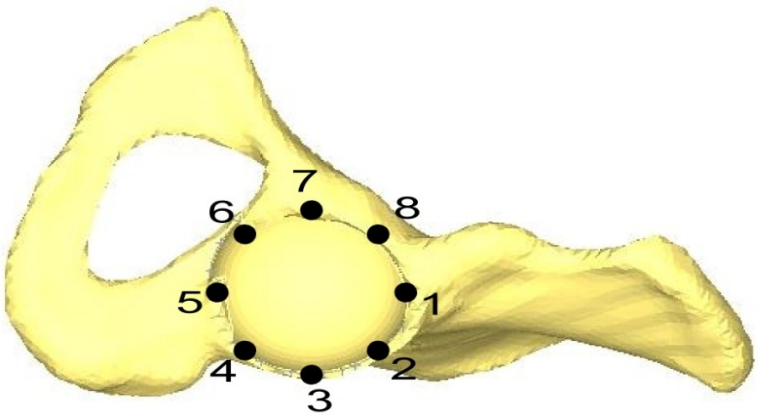

Figure 64 - Position of the Defects. Defects of three sizes were analyzed at position 2 which is bridged and position 7 which is unbridged.

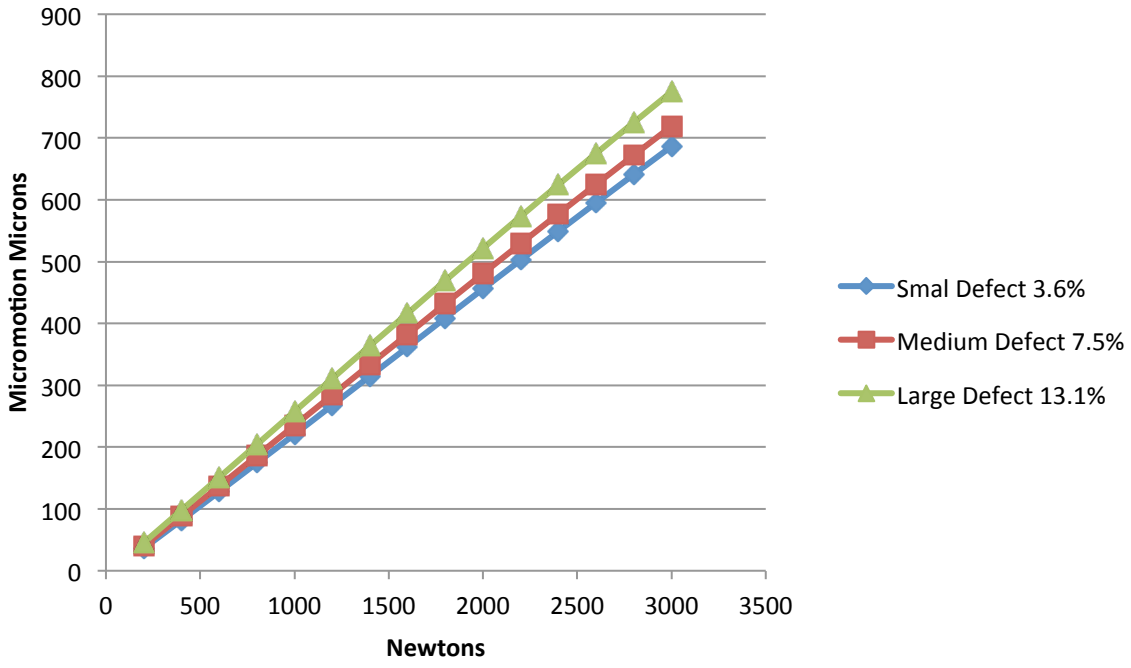

Figure 65 - Defect Size Small Medium and Large Position 7 Non Bridged. An increase in defect size is associated with an increase in micromotion.

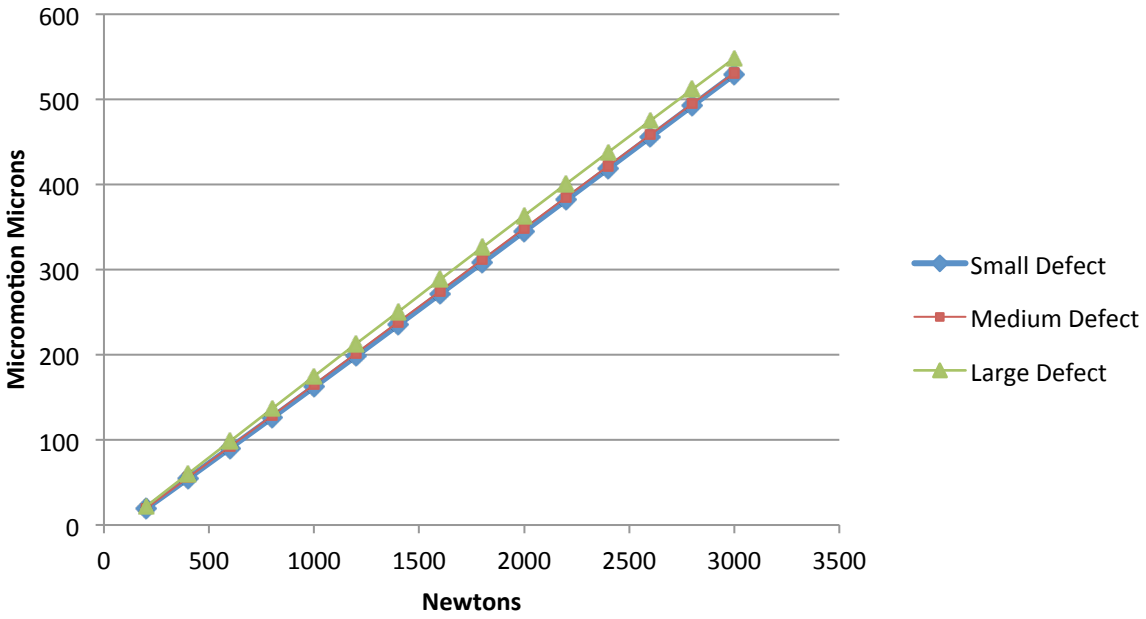

Figure 66 - Defect Size Small Medium and Large Position 2 Bridged. An increase in defect size causes a minimal increase in micromotion

A comparison of the micromotion shows that there is very little difference in the micromotion of the bridged defects even when the defect is almost quadrupled in size (Figure 65). The nonbridged shows significant increases in micromotion associated with an increase of defect size (Figure 66).

The importance of this is clear in acetabular reconstruction. Defect size and location must both be considered when placing an acetabular cup. The prosthesis must if possible bridge and be fixed across defects. An unbridged defect can increase cup micromotion leading to possible instability. Defects that cannot be bridged by the cup can be bridged by using screws or an external plate. The plate can be placed to stabilize the defect prior to placement of the cup.

CHAPTER 14 – Discussion

An evaluation performed of the equatorial bonding of the cup showed that a decrease of the constrained surface can increase cup instability under physiologic loads and possibly lead to cup loosening [70] [71] [72] [73] [74] [75]. Several manufacturers have previously introduced metal on metal cementless cups that had decreased radii. The manufacturers were concerned about metal wear associated with the impingement of the metal prosthetic neck on the rim causing fretting and decreased the radius of the cups. The decreased radius cups were introduced worldwide (Figure 67).

Two issues arose with these cups. First, a significant number of the cups were showing premature unexpected loosening in the first 24 months after implantation. The second issue was metal debris causing a soft tissue reaction associated with global tissue destruction.

The early loosening associated with failure of these cups is probably due to poor initial fixation. The decreased radius cup is analogous to the first scenario of the first experiment (Figure 67).

In this design we would expect friction to be greatest equatorially (Figure 25). There is some elastic deformation to the bone and this would be expected to cause the cup to recoil losing contact at the dome. Decreasing the area of equatorial contact decreases stability of the cup especially to torque. Early micromotion of the cup can preclude bone ingrowth and cause the cup to loosen prematurely.

The dual radius cup also has a decreased equatorial contact area. Our experiments show that a moderate decrease in bonding contact on the dome side of the equator has little effect on cup stability [77]. However larger decreases can cause a substantial decrease in cup stability.

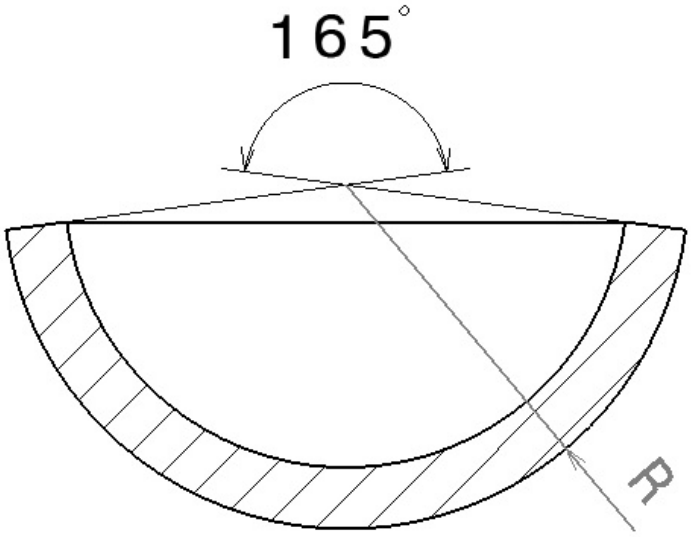

Figure 67 - Decreased radius cup shows decreased equatorial contact. The cup is "cut back" on the equator to diminish impingement of the femoral neck.

Defects of the acetabulum can have different effects on cup stability. The size of defect alone is not sufficient to judge the import of a bone deficiency. In our experiment defects the size of defect made little difference when the defect was outside the anterior or posterior column and bridged by constraining nodes. However when the defect was placed in a column and not bridged by constraining nodes enlargement of the defect was associated with an increase in cup stability.

The third experiment demonstrated that the location of the defect is critical to cup stability. The cementless cup is "wedged" between the anterior columns of the acetabulum. Defects that fall out of the columns both superiorly or inferiorly do not have a substantial effect on cup stability. Defects of the columns themselves tend to be unstable. In scenarios where there

is a lack of support in the anterior or posterior column it behooves the surgeon to use an adjunctive form of fixation such as screws, a custom made flanged cup, or a cup cage construct.

The experiment attempted to mimic the initial condition of implant placement. Clearly the in vivo implant interface has a combination of elastic plastic deformation that is difficult to model. Also this model only looks at the initial condition after implantation. Several authors have attempted to model the bone changes at the interface that are associated with bone modeling [78].

Finite element has been used on a patient specific basis to correct femoral deformity and deformity of the hip joint [79]. In the future finite element may be used to optimize hip revision in cases of severe bone loss.

CHAPTER 15 – Conclusion

The acetabular cup is surrounded by the anterior and posterior columns and the superior dome of the acetabulum. Cup stability is fostered by the anterior and posterior columns. The portion of the acetabulum inferior to the columns is nonstructural Defects of the acetabular rim in the anterior and posterior columns tend to have a destabilizing effect on the micromotion of the acetabulum. These defects have been termed structural defects. Defects that are straight superior or inferior have much less of an effect on destabilizing the acetabulum.

Defects in the columns permit more micromotion of the cup in relation to the bone. This micromotion is critical because in vivo increased micromotion can preclude the ingrowth of bone into a cup. Although in our model the cup is bound about the equator, in vivo a lack of ingrowth will eventually permit complete loosening of the cup. This is then associated with large displacement of the cup and pain. This is treated surgically with cup revision.

Bridged defects where the cup is fixed on either side of the defect are more stable than defects where the cup is only fixed to one side of the defect. Increasing defect size generally increases the micromotion of the cup. This effect is much more apparent in non- bridged than in bridged defects.

When loading an acetabular cup with a bone defect, peak stresses tend to occur at the site of the bone defect. This effect is again magnified in defects that are not bridged by the cup. The unbridged defect can act a stress riser potentially leading to an acetabular fracture. In the scenario of a defect in general the surgeon must avoid high impact forces. The surgeon can also consider stabilizing an unbridged defect with a plate and screws, or screws alone placed through holes in the cup.

Initial fixation of a cementless cup is primarily at the rim of the cup. Decrease radius cups have been designed to decrease femoral neck impingement. In the case of a metal on metal cup impingement of the metal femoral neck can cause significant wear and metallosis. An unexpected result is the decrease in rim contact area. In our model this has lead to increased micromotion that can threaten cup stability. This is reflected in the clinical finding that decreased radius monoblock cups have a relatively high failure rate due to loss of initial fixation.

Dual radius cups have a greater radius at the equator of the cup than at the dome. Fundamentally the reaming is performed to the radius of the dome so that upon insertion the equator is underreamed. Our model demonstrated that decreasing the equatorial portion could also be associated with increased micromotion.

Modeling of the cup bone interface of an acetabulum that is to be reconstructed can provide the surgeon with valuable information on the structural stability of the construct. Further refinement of this technique will allow the surgeon to mechanically optimize the proposed construct prior to performing the actual surgery.

Bibliography

[1] "National Hospital Discharge Survey 2010 Table".

[2] S. Lie, L. Havelin and O. Furnes, "Failure rates for 4762 revision total hip arthroplasties in the Norwegian Arthroplasty Register," *The Journal of Bone and Joint Surgery (Br),* vol. 86B, pp. 504-509, 2004.

[3] N. Mahomed, J. Barrett, J. Katz, C. Phillips, E. Losina, R. Lew, E. Guadagnoli, W. Harris, R. Poss and J. Baron, "Rates and outcomes of Primary and Revision Total Hip Replacement in the United States Medicare Population," *The Journal of Bone and Joint Surgery,* vol. 85, pp. 27-32, 2003.

[4] J. Bobyn, R. Pilliar, H. Cameron and G. Weatherly, "The Optimum Pore Size for the Fixation of Porous Surfaced Metal Implants by the Ingrowth of Bone," *Clin Orthop,* vol. 150, p. 262, 1980.

[5] J. Galante, W. Rostoker, R. Luech and R. Ray, "Sintered Fiber Metal Composites as Basis for Attachment of Implants to Bone," *JBJS,* vol. 53A, p. 101, 1971.

[6] B. S. Ramamurti, T. E. Orr, C. R. Bragdon, J. D. Lowenstein, M. Jasty and W. H. Harris, "Factors Influencing Stability at the Interface Between a Porous Surface and Cancellous Bone: A Finite Element Analysis of a Canine In Vivo Micromotion Experiment," *J. Biomed. Mater. Res.,* vol. 362, pp. 274-280, 1996.

[7] P. Perona, J. Lawrence and W. Paprosky, "Acetabular Micromotion as a Measure of Initial Implant Stability in Primary Hip Arthroplasty," *The Journal of Arthroplasty,* vol. 7, pp. 537-547, 1992.

[8] Y. Kim, J. Callaghan, P. Ahn and T. Brown, "Fracture of the Acetabulum During Insertion ofan Oversized Hemispherical Component," *JBJS,* vol. 77A, pp. 111-117, 1995.

[9] P. Sharkey, W. Hozack, J. Callaghan, Y. Kim, D. Berry and A. Hanssen, "Acetabular Fractures Associated with Cementless Acetabular Component Insertion. A Report of 13 Cases.," *J of Arthroplasty,* vol. 14, pp. 426-431, 1999.

[10] I. Zivkovic, M. Gonzalez and F. Amirouche, "The Effect of Under-Reaming on the Cup/Bone Interface of a Press Fit Hip Replacement," *Journal of Biomedical Engineering,* vol. 132, no. 4, p. 41008, 2010.

[11] C. Won, T. Hearn and M. Tile, "Micromotion of cementless hemispherical acetabular components. Does press-fit need adjunctive screw fixation?," *JBJS,* vol. 77B, pp. 484-489, 1995.

[12] J. Hsu, C. Chang, K. An, M. Zobitz, R. Phimolsarnti, R. Hugate and K. Lai, "Effects of screw eccentricity on the initial stability of the acetabular cup," *Int Orthop,* vol. 31, pp. 451-455, 2007.

[13] J. Hsu, K. Lai, Q. Chen, M. Zobitz, H. Huang, K. An and C. Chang, "The relation between micromotion and screw fixation in acetabular cup," *Comput Methods Programs Biomed,* vol. 84, pp. 34-41, 2006.

[14] S. Small, M. Berend, L. Howard, R. Rogge, C. Buckley and M. Ritter, "High initial stability in porous titanium acetabular cups: a biomechanical study," *J Arthroplasty,* pp. 510-516, 2013.

[15] M. Ries, A. Salehi and J. Shea, "Photoelastic analysis of stresses produced by different acetabular cups," *Clin Orthop,* vol. 369, pp. 165-174, 1999.

[16] B. Olory, E. Havet, A. Gabrion, J. Vernois and P. Mertl, "Comparative in vitro assessment of the primary stability of cementless press-fit acetabular cups," *Acta Orthop Belg.,* vol. 70, pp. 31-37, 2004.

[17] R. M. Pilliar, J. M. Lee and C. Maniatopoulos, "Observations on the Effect of Movement on Bone Ingrowth Into Porous-Surfaced Implants," *Clin. Orthop. Relat. Res.,* vol. 208, pp. 108-113, 1984.

[18] C. R. Bragdon, D. Burke, J. D. Lowenstein, D. O. O'Connor, B. Ramamurti, M. Jasty and W. H. Harris, "Differences in Stiffness of the Interface Between a Cementless Porous Implant and Cancellous Bone In Vivo in Dogs Due to Varying Amounts of Implant Motion," *J. Arthroplasty,* vol. 11, pp. 945-951, 1996.

[19] M. Jasty, C. Bragdon, D. Burke, D. O'Connor, J. Lowenstein and W. H. Harris, "In Vivo Skeletal Responses to Porous-Surfaced Implants Subjected to Small Induced Motions," *J. Bone Jt. Surg.,* vol. 79A, pp. 707-714, 1997.

[20] K. Fehring, J. Owen, A. Kurdin, J. Wayne and W. Jiranek, "Initial Stability of Press-Fit Acetabular Components Under Rotational Forces. J of Arthroplasty," *J of Arthroplasty.,* 18

Oct 2013.

[21] J. Heiner, P. Manley, S. Kohles, M. Ulm, L. Bogart and R. Vanderby Jr., "Ingrowth reduces implant-to-bone relative displacements in canine acetabular prostheses," *J Orthop Res.,* vol. 12, pp. 657-664, 1994.

[22] H. Bereiter, M. Bürgi and B. Rahn, "The temporal behavior of the anchorage of a cement-free implanted acetabular cup in animal experiments," *Orthopade,* vol. 6, pp. 295-300, 1992.

[23] J. Stiehl, E. MacMillan and D. Skrade, "Mechanical Stability of Porous-coated Acetabular Components in Total Hip Arthroplasty," *Journal of Arthroplasty,* vol. 6, pp. 295-300, 1994.

[24] S. Mantell, H. Chanda, J. Bechtold and R. Kylem, "A parametric study of acetabular cup design variables using finite element analysis and statistical design of experiments," *J Biomech Eng.,* vol. 120, pp. 667-675, 1998.

[25] S. Cook, K. Thomas, R. Barrack and T. Whitecloud, "Tissue Growth into Porous Coated Acetabular Components in 42 Patients. Effects of Adjunct Fixation," *Clin Orthop.,* vol. 283, pp. 163-170, 1992.

[26] J. Bobyn, K. Toh, S. Hacking, M. Tanzer and J. Krygier, "Tissue response to porous tantalum acetabular cups: a canine model," *J Arthroplasty,* vol. 14, pp. 347-354, 1999.

[27] D. Sumner, M. Jasty, J. Jacobs, R. Urban, C. Bragdon, W. Harris and J. Galante, "Histology of porous-coated acetabular components. 25 cementless cups retrieved after arthroplasty,"

Acta Orthop Scand., vol. 64, pp. 619-626, 1993.

[28] L. Pidhorz, R. Urban, J. Jacobs, D. Sumner and J. Galante, "A quantitative study of bone and soft tissues in cementless porous-coated acetabular components retrieved at autopsy," *J Arthroplasty,* vol. 8, pp. 213-225, 1993.

[29] C. Sychterz, A. Claus and C. Engh, "What we have learned about long-term cementless fixation from autopsy retrievals," *Clin Orthop,* vol. 405, p. 79, 2002.

[30] T. Nishii, N. Sugano, T. Sakai, K. Haraguchi, K. Ohzono and H. Yoshikawa, "Osteoblastic response to osteoarthrosis of the hip does not predict outcome of cementless cup fixation: 79 patients followed for 5-11 years," *Acta Orthop Scand.,* vol. 72, pp. 343-347, 2001.

[31] R. Wasielewski, D. Galat, K. Sheridan and H. Rubash, "Acetabular anatomy and transacetabular screw fixation at the high hip center," *Clin Orthop,* vol. 438, pp. 171-176, 2005.

[32] M. Dapuzzo and R. Sierra, "Acetabular considerations during total hip arthroplasty for hip dysplasia," *Orthop Clin North Am,* vol. 43, pp. 369-375, 2012.

[33] A. Kamath, P. Evangelista and C. Nelson, "Total hip arthroplasty with porous metal cups following acetabular fracture," *Hip Int.,* vol. 23, pp. 465-471, 2013.

[34] S. Olson and J. Matta, "The computerized tomography subchondral arc: a new method of assessing acetabular articular continuity after fracture (a preliminary report)," *J. Orthop.,* vol. 7, pp. 402-413, 1993.

[35] O. Lubovsky, M. Kreder, D. Wright, A. Kiss, A. Galant, H. Kreder and C. Whyne, "Quantitative measures of damage to subchondral bone are associated with functional outcome following treatment of displaced acetabular fractures," *J Orthop Res.,* vol. 31, pp. 1980-1985, 2013.

[36] D. Clohisy, "Cellular Mechanisms of Osteolysis," *JBJS,* vol. 85, pp. 4-6, 2003.

[37] D. Haynes, T. Crotti, A. Potter, M. Loric, G. Atkins, D. Howie and D. Findlay, "The Osteoclastogenic Molecules RANJL and RANK are Associated with Periprosthetic Osteolysis," *JBJS,* vol. 83B, pp. 902-911, 2000.

[38] N. Kitamura, C. Sychterz-Terefenko and C. Engh, "The Temporal Progression of Pelvic Osteolysis After Uncemented Total Hip Arthroplasty," *Journal of Arthroplasty,* vol. 21, pp. 791-795, 2006.

[39] A. Sternheim, D. Backstein, P. Kuzyk, G. Goshua, Y. Berkovich, O. Safir and A. Gross, "Porous metal revision shells for management of contained acetabular bone defects at a mean follow-up of six years: a comparison between up to 50% bleeding host bone contact and more than 50% contact," *JBJS,* vol. 94B, pp. 158-162, 2012.

[40] W. Paprosky, P. Perona and J. Lawrence, "Acetabular Defect Classification and Surgical Reconstruction in Revision Arthroplasty: A Six Year Follow-Up Evaluation," *J Arthroplasty,* vol. 9, pp. 33-44, 1994.

[41] N. Sheth, C. Nelson, B. Springer, T. Fehring and W. Paprosky, "Acetabuar Bone Loss in Revision Total Hip Arthroplasty: Evaluation and Management," *Journal of AAOS,* vol. 21,

pp. 128-139, 2013.

[42] J. D'Antonio, W. Capello and L. Borden, "Classification and Management of Acetabular Abnormalities in Total Hip," *Clin Orthop,* vol. 243, p. 127, 1989.

[43] G. Wright and W. Paprosky, "Acetabular Reconstruction: Classification of Bone Defects and Treatment Options," in *Surgery of the Hip*, D. Berry and J. Lieberman, Eds., Philadelphia, Elsevier, 2013, pp. 1070-1084.

[44] C. Gozzard, A. Blom and A. Taylor, "A Comparison of the Reliability and Validity of Bone Stock Loss Classification Systems Used for Revision Hip Surgery," *J of Arthroplasty,* vol. 18, pp. 638-642, 2003.

[45] D. Campbell, D. Garbuz and B. Masri, "Reliability of Acetabular Bone Defect Classification Systems in Revision Total Hip Arthroplasty," *J of Arthroplasty,* vol. 16, p. 83, 2001.

[46] W. Kafer, C. Fraitzl, S. Kinkel and S. Kessler, "Analysis of Validity and Reliability of Three Radiographic Classification Systems for Preoperative Assessment of Bone Stock Loss in Revision Total Hip Arthroplasty," *Z Orthop Ihre,* vol. 142, pp. 33-39, 2004.

[47] V. Goldberg, "Selection of bone grafts for revision total hip arthroplasty," *Clin Orthop Relat Res.,* vol. 381, pp. 68-76, Dec 2000.

[48] R. Wasielewski, D. Galat, K. Sheridan and H. Rubash, "Acetabular anatomy and the transacetabular fixation of screws in total hip arthroplasty," *Clin Orthop Relat Res.,* vol.

438, pp. 171-176, 2005.

[49] M. Abolghasemian, S. Tangsataporn, A. Sternheim, D. Backstein, O. Safir and A. Gross, "Porous metal augments: big hopes for big holes," *JBJS,* vol. 95B 11Suppl A, pp. 103-108, 2013.

[50] M. Abolghasemian, S. Tangsataporn, A. Sternheim, D. Backstein, O. Safir and A. Gross, "Combined trabecular metal acetabular shell and augment for acetabular revision with substantial bone loss: a mid-term review," *JBJS,* vol. 95B, pp. 166-172, 2013.

[51] M. Daria and D. Wentz, "Repair of Periprosthetic Pelvis Defects With Porous Metal Implants: A Finite Element Study," *Biomech Eng,* vol. 132, pp. 21006-21012, 2010.

[52] H. Egawa, H. Ho and R. Hopper, "Computed Tomography Assessment of Pelvic Osteolysis and Cup-Lesion Interface Involvement with a Press-Fit Porous-Coated Acetabular Cup," *The Journal of Arthroplasty,* vol. 24, no. 2, 2009.

[53] W. Maloney, P. Herzwurm, W. Paprosky, H. Rubash and C. Engh, "Treatment of Pelvic Osteolysis Associated with a Stable Acetabular Component Inserted without Cement as Part of a Total Hip," *JBJS,* vol. 79A, pp. 1628-1634, 1997.

[54] K. Gustke, M. Levering and M. Miranda, "Use of jumbo cups for revision of acetabulae with large bony defects," *J Arthroplasty,* vol. 29, pp. 199-203, 2014.

[55] P. Lachiewicz and E. Soileau, "Do Jumbo Cups Cause Hip Center Elevation in Revision THA? A Computer Simulation.," *Clin Orthop Relat Res.,* vol. 472, pp. 572-576, 2014.

[56] D. Lakstein, D. Backstein, O. Safir, Y. Kosashvili and A. Gross, "Trabecular Metal Cups for Acetabular Defects With 50% or Less Host Bone Contact," *Clin Orthop Relat Res.,* vol. 467, no. 9, pp. 2318-2324, 2009.

[57] D. Berry, C. Sutherland, R. Trousdale, C. Colwell Jr., H. Chandler, D. Ayres and A. Yashar, "Bilobed oblong porous coated acetabular components in revision total hip arthroplasty," *Clin Orthop Relat Res.,* vol. 371, pp. 154-160, 2000.

[58] P. Abeyta, R. Namba, G. Janku, W. Murray and H. Kim, "Reconstruction of major segmental acetabular defects with an oblong-shaped cementless prosthesis: a long-term outcomes study," *J Arthroplasty,* vol. 23, pp. 247-253, 2008.

[59] Y. Kosashvili, D. Backstein, O. Safir, D. Lakstein and A. Gross, "Acetabular revision using an anti-protrusion (ilio-ischial) cage and trabecular metal acetabular component for severe acetabular bone loss associated with pelvic discontinuity," *JBJS,* vol. 91B, pp. 870-876, 2009.

[60] M. Taunton, T. Fehring, P. Edwards, T. Bernasek, G. Holt and M. Christie, "Pelvic discontinuity treated with custom triflange component: a reliable option," *CORR,* vol. 470, pp. 428-434, 2012.

[61] Z. Li, N. Butala and B. Etheridge, "A Biomechanical Study of Periacetabular Defects and Cement Filling," *Journal of Biomechanical Engineering,* vol. 129, 2007.

[62] P. Lee, G. Raz, O. Safir, D. Backstein and A. Gross, "Long-term Results for Minor Column Allografts in Revision Hip Arthroplasty," *Clin Orthop Relat Res,* vol. 468, pp. 3295-3303,

2010.

[63] D. Jacofsky, J. McCarnley, A. Jaczynski, M. Shrader and M. Jacofsky, "Improving Initial Acetabular Component Stability in Revision Total Hip Arthroplasty Calcium Phosphate Cement vs Reverse Reamed Cancellous Allograft," *J Arthroplasty,* vol. 27, pp. 305-309, 2012.

[64] F. Amirouche, F. Romero, M. Gonzalez and L. Aram, "Study of Micromotion in Modular Acetabular Components During Gait and Subluxation: A Finite Element Investigation," *J Biomech Eng,* vol. 103:021002, 2008.

[65] F. Romero, F. Amirouche, L. Aram and M. Gonzalez, "Experimental and analytical validation of a modular acetabular prosthesis in total hip arthroplasty," *J Orthop Surg Res.,* vol. 16, pp. 2-7, 2007.

[66] G. Bergmann, F. Graichen and A. Rohlmann, "Hip joint loading during walking and running, measured in two patients," *J Biomech,* vol. 26, pp. 969-990, 1993.

[67] B. Stansfield and A. Nicol, "Hip Contact Forces in Normal Subjects and Subjects with Total Hip Prosthesis," *Clinical Biomechanics,* vol. 17, pp. 130-139, 2002.

[68] P. Brooks, "Dislocation following total hip replacement: causes and cures," *Bone Joint J.,* vol. 95B Suppl A, pp. 67-69, 2013.

[69] M. Gonzalez, R. Carr, S. Walton and W. Mihalko, "The evolution and modern use of metal-on-metal bearings in total hip arthroplasty," *Instr Course Lect.,* vol. 60, pp. 247-255, 2011.

[70] S. Shemesh, Y. Kosashvili, S. Heller, E. Sidon, L. Yaari, N. Cohen and S. Velkes, "Hip arthroplasty with the articular surface replacement (ASR) system: survivorship analysis and functional outcomes," *Eur J Orthop Surg Traumatol,* vol. 11, 2013.

[71] N. Bernthal, P. Celestre, A. Stavrakis, J. Ludington and D. Oakes, "Disappointing short-term results with the DePuy ASR XL metal-on-metal total hip arthroplasty," *J Arthroplasty,* vol. 27, pp. 539-544, 2012.

[72] M. Althuizen, M. Hooff, S. vdBerg-v Erp, J. Limbeek and M. Nijhof, "Early failures in large head metal-on-metal total hip arthroplasty," *Hip Int,* vol. 22, pp. 641-647, 2012.

[73] J. Mokka, K. Mäkelä, P. Virolainen, V. Remes, P. Pulkkinen and A. Eskelinen, "Cementless Total Hip Arthroplasty with Large Diameter Metal-on-Metal Heads: Short-Term Survivorship of 8059 Hips from the Finnish Arthroplasty Register," *Scand J Surg,* vol. 102, pp. 117-123, 2013.

[74] G. Steele, T. Fehring, S. Odum, A. Dennos and M. Nadaud, "Early failure of articular surface replacement XL total hip arthroplasty," *J Arthroplasty,* vol. 26, no. 6 Suppl, pp. 14-18, 2011.

[75] W. Long, M. Dastane, M. Harris, Z. Wan and L. Dorr, "Failure of the Durom Metasul acetabular component," *Clin Orthop.,* vol. 468, no. 2, pp. 400-405, 2010.

[76] F. Amirouche, Y. Gussous, W. Goldstein, M. Gonzalez and S. Broviak, "Augmentation of Acetabular defect with Kryptonite Bone Cement in Total Hip Replacement A Mechanical Testing of Micromotion and Stability of Cup/Bone Interface," in *Orthopedic Research*

Society Annual Meeting, Long Beach CA., January 2011.

[77] E. Bonicoli, A. Baluganti, L. Andreani, N. Piolanti and M. Lisanti, "The dual radius hemispherical 'Trident" cup: results based on 150 consecutive cases," *Surg Technol Int,* vol. 22, pp. 229-235, 2012.

[78] M. Tarala, D. Janssen and N. Verdonschot, "Toward a Method to Simulate the Process of Bone Ingrowth in THA using Finite Element Method," *Med Eng Phys,* vol. 35, pp. 543-548, 2013.

[79] K. Rhyu, Y. Kim, W. Park, K. Kim, T.-J. Cho and I. Choi, "Application of finite element analysis in pre-operative planning for deformity correction of abnormal hip joints - a case series," *Proc Inst Mech Eng H,* vol. 225, pp. 929-936, 2011.

APPENDIX I – MIMICS Model

Section 1: Import and Thresholding

Open

File

Import images

Dicom Images (CT scan)

Next

Convert

Ok

Segmentation

Thresholding

Bone scale

Apply

Segmentation

Multiple slice edit

Lasso- axial-remove

Zoom to full screen

Box

400% magnification

Lasso and then apply to remove any connection between segments

Crop mask

Ok

Segmentation

Region growing

3D objects

New

Latest mask

Calculate

Tools

Wrap

Specify parameters: closing distance size of hole to be closed smallest detail coarseness (measure distance in tool bar) (3,5)

Tools

Smoothing 0.5

Section 2: Import into 3MATIC and Placement of Reamer

Click on 3d image

3matic environment- current mask

Remesh icon on right second row

file

import cup reamer handle assembly

file

import block made from actual pelvis with inserted cup

edit

N Points Registration

Fixed Entity Pelvis

moving points: cup reamer

apply

edit

use rotation function and inertial coordinates to place cup reamer

use linear translation function and inertial coordinates to place cup reamer

reamer must be in position defined by the block

Section 3: CAD Reaming and Placement of Acetabular Cup

Boolean Subtraction

expert mode on (at bottom mid screen)

Click create new part

Unclick remove original

entity

pelvis

subtraction entity

cup

apply

Mark

3d lasso

delete reamer portion of assembly

translate cup along z axis so that cup is just touching rim (remember cup is 1mm greater in diameter than reamer)

view

create section

2points and a plane (datum plane)

repeat to create perpendicular sections

Translate cup along major axis so cup is touching rim of cup slight protrusion less than 1mm is preferable

use cross section function in multiple planes to check position of cup

create duplicate of cup and reamer

create real cross section using a primitive plane and CAD boolean cut function

measure distance of cup from apex (usually about 17.5 mm)

Delete all cross sections and duplicates

Section 4: Meshing

Data Base Tree

Highlight pelvis

view

filled with triangle edges (ICON)

Fixing

Reduce

Geometrical Error .05

Number of iterations 5

Apply

Remeshing

Create inspection scene

Color low quality triangles

Shape measure 0-0.3

height over base 0.3

RinRout (N)- HeightBase N

Largest Angle A

Maximum Minimum 0.3

Auto remesh

Quality threshold 0.3

Maximum geometrical error 0.15 (remember higher geometrical error allows increased change in surface)

Control max triangle edge

10.00

12 iterations

preserve surface contour

apply

remeshing

Database tree

highlight cup icon on the right

create inspection scene

color low quality triangles

height over base 0.3

RinRout (N)- HeightBase N

Largest AngleA

Maximum Minimum 0.3

auto remesh

Quality threshold 0.3

maximum geometrical 0.15 (remember higher geometrical error allows increased change in surface)

Control max triangle e

10.000

12 iterations

preserve surface contour

apply

Database Tree

highlight cup icon on the right

Create volume Mesh

Control edge length

Maximum edge length 3.5

Aspect Ratio A

25.00

Apply

Database Tree

Select Pelvis Icon on the right

Create volume Mesh

Control edge length

Maximum edge length 3.5

Aspect Ratio A

25.00

Apply

Section 5: Transfer to MIMICS Final Thresholding and Prepare for Export into ANSYS

control v cup

control c cup

control v pelvis

control c

masks

create new masks

threshold

compact bone adult

apply

masks

create new mask

threshold

spongiosa bone adult

add custom increase in grey value

apply

FEA mesh on right

highlight pelvis

material properties (3dots)

mask

select masks

select the cortical and spongiosa (custom Masks)

material editor

cortical 5600 0.3

Spongiosa 500 0.3

ok

fea mesh

cup

material assignment (3dots)

uniform

number of materials 1

material editor

100000 0.3

ok

export

ANSYS

mesh

pick pelvis and cup

add

select destination

ok

APPENDIX II – ANSYS Finite Element Routine

Section 1: Import into ANSYS - Material Properties

Import into ANSYS (cdb file from Mimics)

Import cup

Preprocessor

Numbering controls

Add num offset

300,000

Offset (nodes, elements, material material properties)

close

Select

Component manager

Rename components

Read input from pelvis

Select

Component manager

Rename components (Pelvis, Acetabulum, Cup and Inserter)

Preprocessor

Material properties

Material models

Material (check all the material models here)

Apply Properties to any materials not carried over from MIMICS

New model (upper left corner)

Structural

Friction Coefficient

0.6 - 0.8

apply

close

Select (at top to the left of File))

Select Everything

Select (at the top to the left of File)

Component Manager

Select Cup and Inserter

Check select and display

Select (at the top to the left of File)

Entities

Nodes

By num pick

Reselect

Ok

On left pop up

Select box

Use box to select nodes of cup only

Component Manager select create component

Name component cup and base

Component Manager

Click on “cup and base”

Check select and display “cup and base”

Select (at the top to the left of File)

Entities

Nodes

By num pick

Reselect

Ok

On left pop up

Select box

Use box to select nodes of cup minus base only

Component Manager select create component

Name component cup minus base

Component Manager

Click on “cup and base”

Check select and display “cup and base”

Select (at the top to the left of File)

Entities

Nodes

By num pick

Reselect

Ok

On left pop up

Select box

Use box to select nodes of base only

Component Manager select create component

Name component base

Click on “base”

Check select and display “base”

Select (at the top to the left of File)

Entities

Nodes

By num pick

Reselect

Ok

On left pop up

Select box

Use box to select nodes of base rim only

Component Manager select create component

Name component base rim

Click on “base rim and ” “cup without base” (hint depress control button on keyboard to select both)

Check select and display

Select (at the top to the left of File)

Entities

Nodes

By num pick

Reselect

Ok

On left pop up

Select box

Use box to select nodes of base rim and cup without base (this should be all nodes pictured)

Component Manager select create component

Name component “cup and rim

select everything

Section 2: Contact

preprocessor

contact manager

contact wizard

target type flexible

target surface cup

next

surface to surface

“cup and rim”

optional settings

Basic

Normal Penalty Stiffness 1.0

Penetration Tolerance 0.1

Pinball Region: Auto

Contact Stiffness each iteration (Pair ID Based)

Contact Algorithm : Augmented LaGrange Method

Contact Detection on Gauss Point

Behavior Contact Surface Standard

Friction

Material ID (from component manager)

0.6-0.8

instant adjustment

Initial Penetration Include everything

close gap and reduce penetration or ICONT

Contact surface offset : 0

next

Section 3: Load Step

create

work plane (at top)

local coordinate system

create local CS

by three nodes

select 3 odes on base plane of inserter

create local cs “11”

preprocessor

modeling

move / modify

transfer coordinates

nodes

Pick all

KCNTO = 0

INC= 0

Work plane

change active CS to global cartesian

change display to global cartesian

Solution

Define Loads

Apply

Structural

Displacement

On Nodes

Box

Constrain pelvis x,y,z

Inserter push in z direction (measured in MIMICS)

Inserter Constrain x,y

Solution

Load Step Options

Write LS File (1)

Solution

Define Loads

Delete

Structural

Displacement

On Nodes

Box

Delete all constraints on inserter but not on pelvis

Solution

Load Step Options

Write LS File (2)

Solution

Define Loads

Apply

Structural

Force/ Moment

On Nodes

Apply loading force to selected nodes

Solution

Load Step Options

Write LS File (3)

Solution

Analysis Type

Sol'n Controls

0,0,0

Write every substep

Section 4 Solution and Results

Solve

From LS Files

Start 1

End 3

Increment 1

ok

read results by load step

plot results

deformed shape

Abbreviated Curriculum Vitae

Mark H. Gonzalez M.D., M.Eng.

Education
B.S. Biochemistry: University of Illinois Urbana Champaign 9-1974 to 6-1976
M.D. University of Chicago 8-1976- to 6-1980
Residency Orthopedic Surgery, University of Illinois 8-1980- to 6-1985
Fellowship Hand Surgery, Michigan State 7-1985 to 1-1986
Fellowship Total Joint Replacement, Ohio State University 1-1986 to 6-1986
Fellowship Hand Surgery, University of Louisville 7-1986 to 6-1987
Masters in Engineering, University of Illinois at Chicago 6-2004

Academic Appointments
The Riad Barmada Endowed Professor in Orthopedic Surgery
University of Illinois 1-2008 to present
Chairman of Orthopedic Surgery, University of Illinois 3-2007 to present
Professor of Orthopedic Surgery, University of Illinois
Chairman of Orthopedic Surgery Stroger Hospital of Cook County 12-1999 to 7-2009

Selected Publications

Amirouche F, Choi KW, Goldstein W, Gonzalez MH, Broviak S: Finite Element Analysis of Resurfacing Depth and Obliquity on Patella Stress and Stability in TKA. Journal Of Arthroplasty 28:978-984, 2013.

Chow JC, Sensinger J, McNeal D, Chow B, Amirouche F, Gonzalez MH, The Importance of Proximal A2 and A4 Pulleys to Maintaining Kinematics in the Hand: A Biomechanical Study. Accepted The Hand 2-2013.

Chow JC, Sensinger J, McNeal D, Chow B, Amirouche F, Gonzalez MH, The Importance of Proximal A2 and A4 Pulleys to Maintaining Kinematics in the Hand: A Biomechanical Study. Accepted The Hand 2-2013.

Amirouche F, Gonzalez MH, Hilton K , Chandran N, Barmada R, Goldstein W. Optimization of the Posterior Stabilized Tibial Post for Greater Femoral Rollback after Total Knee Arthoplasty - A Finite Element Analysis. International Orthopedics 33:687-692, 2008.

Zivkovich I, Gonzalez MH, Amirouche F. The Effect of Under –Reaming on the Cup/Bone Interface of a Press Fit Hip Replacement. Journal of Biomechanical Engineering 132: 41008, 2010.

Amirouche F, Romero F, Gonzalez MH, Aram L. Study of Micromotion in Modular Acetabular Components during Gait and Subluxation. A Finite Element Investigation. Journal of Biomechanical Engineering 130: 021002, 2008.